



AUSTRIAN
MARSHALL PLAN FOUNDATION
VIENNA | AUSTRIA

Marshall Plan Scholarship Paper

Viktor Konakovsky

Vienna University of Technology

(Vienna, Austria)



University of Minnesota

(Minneapolis, Minnesota, USA)



Advisors:

Wei Shou Hu, Ph.D.

Univ.Prof. Dipl.-Ing. Dr.techn.Christoph Herwig

2015

Improved metabolic process control by analysis of genetic clone background in mammalian cell culture

Viktor Konakovsky^{1‡}, Tung Le^{2‡}, Andrew Yongky², Ravali Raju², Nandita Vishvanathan², Christoph Herwig¹, Wei Shou Hu²

¹ Institute of Chemical Engineering, Division of Biochemical Engineering, Vienna University of Technology, Gumpendorfer Strasse 1A 166-4, 1060, Vienna, Austria,

E-mails: konak004@umn.edu, christoph.herwig@tuwien.ac.at

² Department of Chemical Engineering and Materials Science, University of Minnesota, 421 Washington Avenue SE, Minneapolis, MN 55455-0132 USA

[‡] These Authors contributed equally to this work.

E-mails: acre@cems.umn.edu

Abstract

Currently, the analysis of mammalian cell culture bioprocesses is discriminated into a multitude of highly complex disciplines which share several common goals: to make bioprocesses safer, cheaper and easier to control. In mammalian fed-batch process control, one topic has been dominating and dictating research in this area for many years: The problem in build-up of high lactic acid concentrations [1].

Interdisciplinary discoveries in several fields are able to combine and expand knowledge in the individual technologies and address today's challenges in industry [2][3]. We present a systems approach comprising process control, modeling and cell line engineering, where the genetic background of mammalian cells and tissues, more precisely their measured transcript level and isoform composition, is linked to a highly customizable mathematical model. This model can be used to test the cell's *in-silico* behavior in various process modes and simulate the metabolic response under physiological conditions. One of the targets of modeling was to show different pathways how to reduce lactic acid build-up and to explore the model to gather new ideas to accomplish this in different ways. By incorporation of the clone's genetic identity we i) show differences in the dynamics of metabolic shifts ii) reveal potential targets to improve cell engineering and iii) provide the basis for screening suitable process and control modes for potential production cell lines *ab initio* [4].

Keywords: mammalian cell culture, systems analysis, mathematical modeling, CHO cell metabolism, process control

1. Introduction

1.1. Problem statement

In process development, clones need to be selected. The main selection criteria for this are high titers and high growth kinetics. However high growth kinetics reveal overflow metabolism, such as lactate production [5][6], which is a disadvantageous in respect to metabolic efficiency [7][8] which often corresponds to a lower product titer [9]. This metabolic efficiency can be modulated by operating in a chemical environment of high productivity and metabolic efficiency, and the tool to do this is using intelligent process control. The challenge we face is that the genetic background of every producing cell line is unique, and their response to one process scenario and its control may be very different. This leads to a different performance under the same chemical conditions and therefore unpredictability and insecurity in regard to the question which conditions may lead to optimal performance *in situ*.

As a consequence, we wish to contribute to an area of hardly any understanding, namely i) how the genetic heritage of clones, more precisely isoform composition, can affect cell metabolism, and ii) how process conditions, such as timing and intensity of shifts or pulses, can lead to a modification of metabolism. Apart from the enzymatic composition, which determines the genetic architecture, the up- or down-regulation in transcriptomic levels [10] can be considered as well to reveal how a stronger transcription may contribute to metabolic regulations. Different tissues, cell lines or high and low producers of the same product can then be analyzed under the same standards and by exposure to identical *in silico* process conditions to find i.e. that a carbon limitation strategy may be beneficial for one clone but not for another due to a general lower glucose uptake rate due to genetic background.

Usually, enough data is available way ahead of the first bioreactor run in form of transcriptomics which analyzed how well the genetic modifications on the clone were integrated. Exactly this data is highly interesting for us and was used to describe particular clone-dependent behavior in simulations. Transcriptomic data from different clones and tissues is publicly available and the model we use for these simulations is based on work published under [8][11][12].

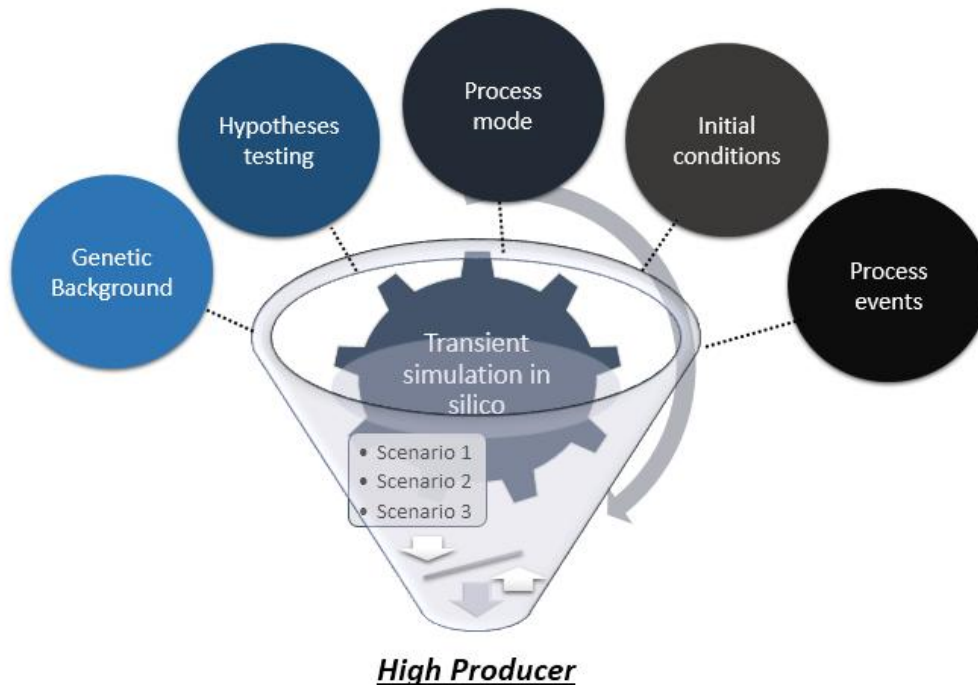


Figure 1: What makes a high producer a high producer?

Each clone reacts differently to process changes. Anticipating these changes by simulating how the real process might possibly run under the given conditions *in silico*, we believe that this tools may help us in finding clone-dependent optimal operating conditions.

1.2. State of the art

Modeling the intricate metabolic behavior of living microorganisms is a challenge which is faced best with as few assumptions a possible. Those which have to be made should be as general and reasonable as possible, optimally without empirical equations and supported by relevant literature. But the most important consideration should be to generate a model which will be able to describe the current problem appropriately. That includes the premise that the given system will fulfill the assumptions most of the time, and this might be the hardest task.

There are many published mathematical models which use mass balances to describe input and output but often a simple model means hefty assumptions which run the danger of having to be recalculated in a parameter estimation fit every single time the model is tested with new data. Such models often include very specific parameters concerning cell growth and death and changing metabolic yields and may lack transferability to other processes because recalibration may not be successful.

The general structure of current mathematical models can be described with Monod-Wyman-Changeaux [13] kinetics, where a rate decreases with a lower concentration of the limiting substrate,

$$r = r_{max} \cdot \frac{C_A}{K + C_A} \quad (1)$$

where r is the forward or backward rate, r_{max} the maximum possible rate, C metabolite concentration of compound A and K the concentration at which the speed of the reaction assumes exactly half maximum speed. Most rate changes, i.e. for metabolite consumption, but even growth rate are described with variants of this relationship. It does not come as a surprise that mostly batch fermentations, but also continuous cultivations can be sufficiently described with variants of this basic relationship and enjoy a great popularity because they work for their intended purpose [14][15]. While in a batch culture the substrate will eventually reach zero, and uptake must stop, in continuous cultivations a particular concentration can be held, and a certain flux can be therefore set up and ensured.

All of these rates involve a forward (fw) and a backward (bw) reaction, therefore each of the reactions r can be written as r_{fw} and r_{bw} [16]. Both rates go into opposite directions, and the resulting final rate determines in which direction the reaction is headed and if a substance is produced or consumed. However, there is more to it, especially if multiple intermediates are involved and the reactions are close to equilibrium. The denominator N explains allosteric regulations which happen further downstream in the equations and can contain several activators and inhibitors which affect the final outcome significantly.

$$r = \frac{r_{fw} - r_{bw}}{N} \quad (2)$$

The full term may look in a simple form as the following equation 3, however the appendix will contain a list of much more complex reactions:

$$r = \frac{r_{fw} \cdot \frac{C_A}{K} - r_{bw} \cdot \frac{C_B}{K}}{1 + \frac{C_A}{K} + \frac{C_B}{K}} \quad (3)$$

Mathematical models often use these kind of descriptions in their equations. They are our best mechanistic attempt to simplify complex effects such as cell growth in batch and fed-batch [17][18][19], but also chemostat cultivations [20][7][21]. There are plenty of models available which extend the simple models by inclusion of parts of the TCA cycle [22][23][24] to gain even more insights into the mechanisms involved, but as more parameters are introduced, complexity level increases while general validity decreases because often the parameters become bound to one clone or process strategy.

In the end, all models may have to prove themselves by showing their practical use in the intended application. Most mammalian processes today are “simple” fed-batches in which cell death is prevented as long as possible by shifts in the external conditions [25] and genetic architecture of the cells [26]. Differences between clones make a generalization of a simple model difficult and may lead to the situation where even after validation in one process the benefit of application is restricted to only this one clone, one type of medium, one type of process condition or all those points at the same time.

Therefore, oversimplified models trying to describe fed-batch cultivation processes might or might not capture enough of the most critical parameters in a dynamic fermentation. To make things even more difficult, an inevitable decrease in cell viability over time massively affects the cell’s metabolism [27][28][29]. The inability to provide a valid and general metabolic model for mammalian processes is symbolized by the huge numbers of different and at the same time similar attempts to reduce a model down to its most essential parts, as summarized by Pörtner et al. [30]. This problem is even more accentuated by the striking lack of mathematical descriptors of critical factors, which influence cell metabolism in a dynamic fermentation format such as batches and fed-batches, where the lack of parameters only shows in the longer fed-batch processes where metabolism is very hard to represent accurately.

Such missing parameters may involve the dynamic changes in pH and pCO₂, which are not always perfectly controlled and osmolality, which is usually not controlled at all in fed-batches [31][32][32]. Homeostasis between external and internal pH, like in lactic acid bacteria [33], is rarely mechanistically considered, although practitioners and researchers know that a shift in external pH shift leads often to a shift in internal pH within less than half an hour [34][35][36] and makes it possible to act directly on the cell’s metabolism [37][38][39][40] by affecting the reaction rate of glycolytic and other enzymes [41][42][43][44].

And yet there is still an insatiable hunger for more simple, universal and accurate models. Because they can be only as good as their assumptions, the premises and expectations of the model’s result should be stated in advance and compared to what is scientifically reasonable to model accurately and what is not. This concerns the following most important factors: i) predictable cell growth and ii) no delayed time effects affecting metabolism. These two conditions hold mostly true for two process formats: short-term batch fermentations and continuous cultivations, in which the chemical environment is refreshed continuously and guarantees stable growth conditions without limitations or inhibitions for a long time. The currently presented model is capable of mimicking all process modes but was intended to mainly generate knowledge from the cell’s genetic architecture and isoform specific mechanism under different chemical conditions.

Pulses in a low glucose environment as well as shifts in pH can lead to different responses between clones and tissues which can be analyzed qualitatively and assessed quantitatively in experiments. Enzyme parameters, sensitivities towards inhibitory and activating substrates as well as any initial metabolic environment can be fully edited and tested under any thinkable range of simulation conditions, and provide interesting insights into the cell’s response to stimuli.

A computer simulation also has a significant advantage over wet lab experiments: the environment is not influenced by any unintended process events which may modify the cells' behavior and can be tested as many times as necessary for the intended purpose by applying minute changes to the process conditions or enzymatic regulation.

Our purpose is to provide a useful tool to improve the understanding in a systems approach in several engineering disciplines [45]. We combine rational protein design, cell clone engineering and accelerated process development by exposing the cells *in silico* to a relevant challenge in several scenarios as described by Kitano [46]. We want to make clear that we do not actually design or modify real proteins in this contribution. We are merely interested in the results of the simulation after protein modification. Such a modification may involve, for instance, substitution of one or several amino acids, which can affect the protein's binding specificity to i.e. a substrate, activator or inhibitor [47][48]. We also advise to remain cautious about the model's qualitative dry lab output which may have to be adapted to the quantitative wet lab reality.

1.3. Approach

Our approach in improving current process control strategies encompasses a mechanistic explanation for differences in clone metabolism based on the clone's genetic background. In order to investigate the differences, the already existing mechanistic model developed by [7][49] was fed clone-specific transcript data [12]. The previously described model is extended by isozyme-specific parameters which are retrieved from literature databases [50][51]. Enzyme levels and ratios can be exploratory varied to find those enzymes which have the largest impact and help to explain most of the in-silico metabolic behavior of the culture. Additionally, a simulation can be conducted in several possible cultivation scenarios, in which metabolic response and clone performance can be assessed *in silico*.

The underlying model was modified and extended in the following respects:

- The most important allosteric regulations happen in glycolysis, therefore the TCA Cycle and PPP were kept constant to prevent over-complication of the given problem [49].
- Isoform fractions of not only a few selected, but all isoforms in the reaction network catalyzing the same reaction are introduced in the rate equations to account for the genetic diversity of clones. The list is incomplete and can be further expanded when feedback regulations in the form of equations become better understood and their kinetic parameters become known.
- Differences in transcript level are used to increase or decrease the calculated rate r_{max} , which opens up simulations of the metabolic response related to variable enzyme levels.
- External process parameters can be varied (i.e. timing and power of shifts in pH, glucose and lactic acid concentration) during simulation to elucidate their implication on cell metabolism and process control [4].

- Several optional settings, i.e. pH sensitivity of glycolytic flux and effect of low glycolytic flux on growth are implemented but not validated, and therefore open for exploration only. We hope they may help in calibrating the model to real data sets in the future.
- The code, originally written in Matlab, is now partially editable in Microsoft Excel, which makes it easier to implement changes on genetic composition, protein mechanism or process control level. Matlab is still required to run the script, but it accesses all previously modified parameters from Microsoft Excel, runs the simulations under the new conditions and saves a report file together with figures of the results.

1.4. Novelty

To the author's knowledge, a clone's full genetic information was never attempted to be included in simulations of its metabolism. We want to focus on the impact of enzyme composition involved in the glycolytic pathway. The simulations are expected to unveil clone-specific responses to dynamic perturbations in the chemical environment as seen in real processes. The individual responses after exposure to different stimuli (glucose pulse, pH shift) are believed to lead to more knowledge in the fields of directed protein design, clone engineering and radical improvements of cell-specific process parameter set-points instead of current arbitrary initial guesses as practiced when characterizing a new clone in industry.

The novelty of this approach is the combination of transcriptomic data, modeling and process control strategies in mammalian cell culture, thus enabling simulation and possibly prediction of the dynamic behavior of different industrial mammalian cell lines and tissues based solely on their genetic background with a mechanistic model. As tangible output qualitative information about an unknown clone's metabolism may be obtained in comparison with another clone such as: strong or weak producer of lactic acid under standard conditions, or good or bad growth under glucose-limited conditions. However, these statements are indicated in the simulations, not in wet lab experiments yet. Therefore, a small part of very differently behaving clones *in silico* should be used for verification of these hypotheses under standardized conditions. This may mean that an industrial strain will leave its proprietary feed and medium environment and may not have the same quantitative behavior as during simulation, but a qualitative analysis should be generally possible.

1.5. Goal

This contribution is dedicated to developing a comprehensive understanding how different isozyme compositions can affect the metabolic fate of a cell line in development and its resulting underlying process control strategy. Such a fate can encompass i.e. metabolic overflow as described by [24][52] or more efficient metabolism [53][54][55]. As simplified representation, the simulations are understood to be qualitative rather than quantitative in their output and serve as a guide to develop lean clones by identifying crucial metabolic regulations and bottlenecks as well as show the path to improvements in

clone engineering and process control in a very early screening of clones. As very practical outcome, this work can be immediately used to screen large data sets of yet untested next-generation high producers [10][12][56] to compare their performance in several synthetic benchmarking scenarios [57].

1.6. Workflow

These process parameters include, but are not limited to pH, substrate and metabolite concentrations, online set-point controls as well as the type of feeding profile [58][59]. Our simplified mechanistic model for glycolysis under different levels and types of isoforms is expected to illuminate the intricate allosteric regulations and dynamic effects of genetically very differently tuned industrial strains and empower process engineers to select the best-suited process control strategy by design.

This contribution is expected to weld the invisible band between cell characteristics on the genomic level, description thereof by mathematical modeling, and final implementation in the bioreactor with state-of-the-art process control. We believe that a holistic perspective is not only capable but also necessary to solve otherwise isolated and therefore challenging problems with the most simple and intuitive techniques from either technology. Our vision is the description of a systematic methodology which may serve as a prototype to describe more complex problems than lactic acid metabolism in the future by bridging several disciplines in bioprocess development [3][60][61].

2. Materials and Methods

2.1. Data set

The available dataset includes different tissues and cell lines and was collected and kindly provided by Nandita Vishvanathan and Ravali Raju [12]. Transcriptomic information was obtained by RNA-seq and microarray measurements of different specimen after 4 and 7 days in culture [10].

2.2. Isoform influence

The levels of each class were statistically analyzed for the min, mean and max values of all clones. The weight of each isoform was calculated for ratios. If only one isoform exists, the ratio is 1, or 100%. An example is given below. The rate multiplies by this ratio and all involved isoforms are added up to determine the final rate. In a simplified example, where rHK1 would weight 0,77 and rHK2 0,21, the final rate calculation would follow the form $r = rHK1 + rHK2$. The differences between both enzymes is their specificity towards glucose, which is closer described in the excel sheet containing all isoform-specific parameters, can be fully modified and serves as direct input for the simulations.

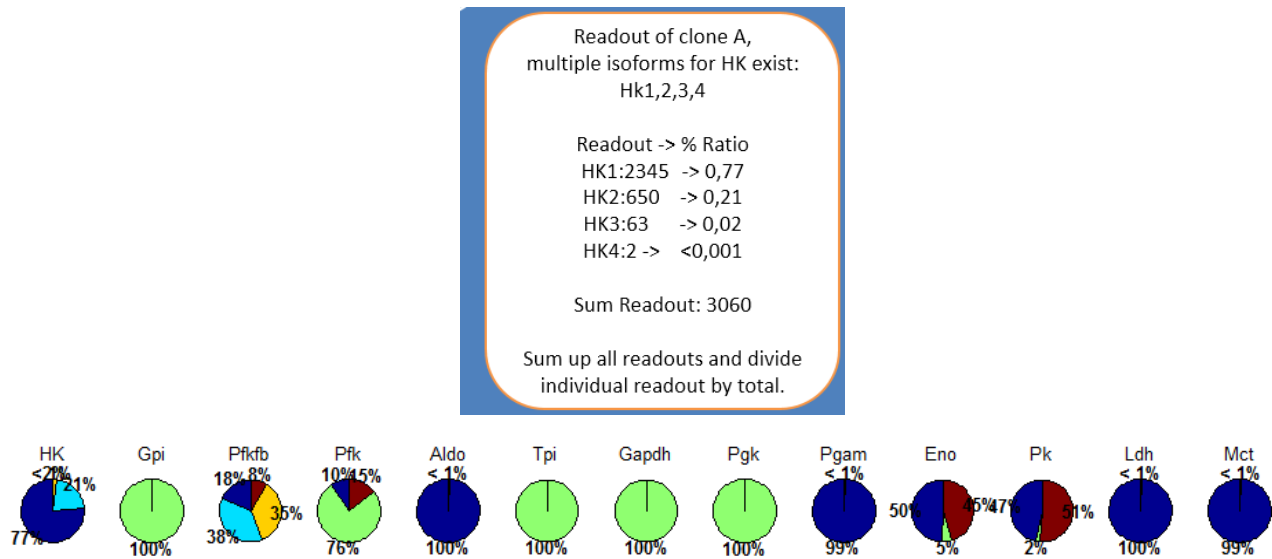


Figure 2: Isoform ratios. Every pie represents a clone’s genetic isoform composition in percent.

2.3. Transcript level normalization

The data was normalized by dividing the genes’ absolute intensity of the readout by the level of a house-keeping gene, whose abundance is assumed to be evenly distributed among the cell lines under investigation and in this case Gapdh [62][63]. The factor (how much more of one particular isoform exists than average) can be then plotted for each isoform and each clone.

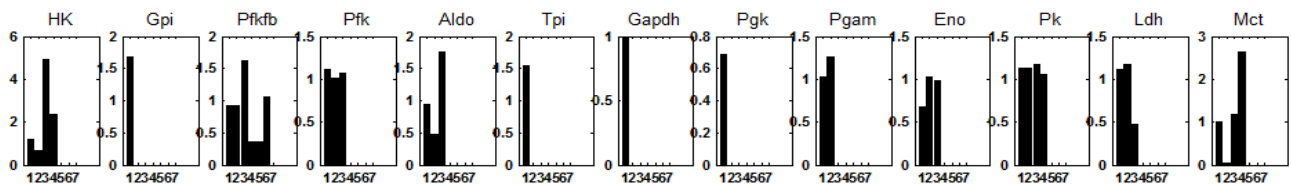
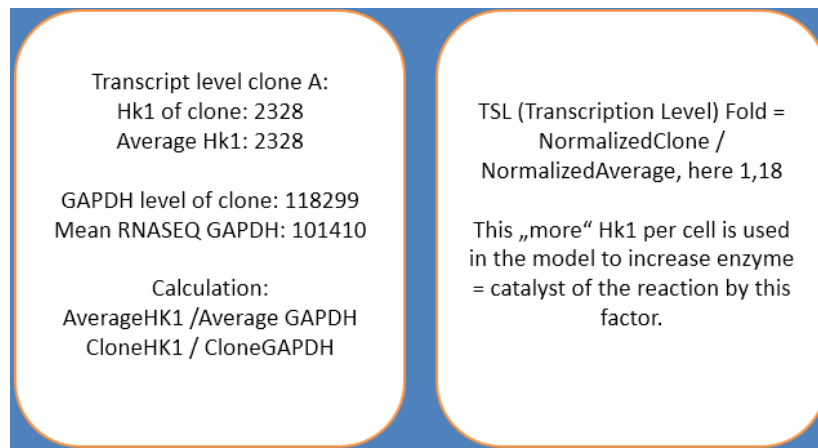


Figure 3: Transcript levels. Every bar represents a clone’s fold-change compared to the mean transcript level of all clones of this isoform.

Finally, the data is automatically read out by Matlab and used for simulation conditions which can be closer specified in the excel sheet containing the starting parameters.

3. Results

3.1. Scenarios

The following scenarios were compiled to test the given dataset under all kinds of different process conditions and to show the difference in metabolic response.

- Impact of clone architecture to model behavior (considering isoform and transcript level)
- Continuous feeding with pH shifts and glucose pulses
- Varying power, direction and timing of pH shifts
- Exploring interesting targets for protein design (*in-silico* modification of substrate/inhibitor binding specificity of i.e. LDH, HK...)

3.2. Simulation of continuous behavior

The following experiments were performed to show the effect of isozyme composition and transcript level on metabolic behavior between different clones.

First, the scenario entails a glucose shift from a strongly limiting concentration of 0,1 mM glucose to 5,4 mM (roughly 1 g/L) glucose. On the left, glucose concentration in mM is shown, on the right the specific glucose consumption rate of the cells in mM/h. As can be seen in this very simple example, a change in glucose concentration leads to an instant increase in the consumption rate.

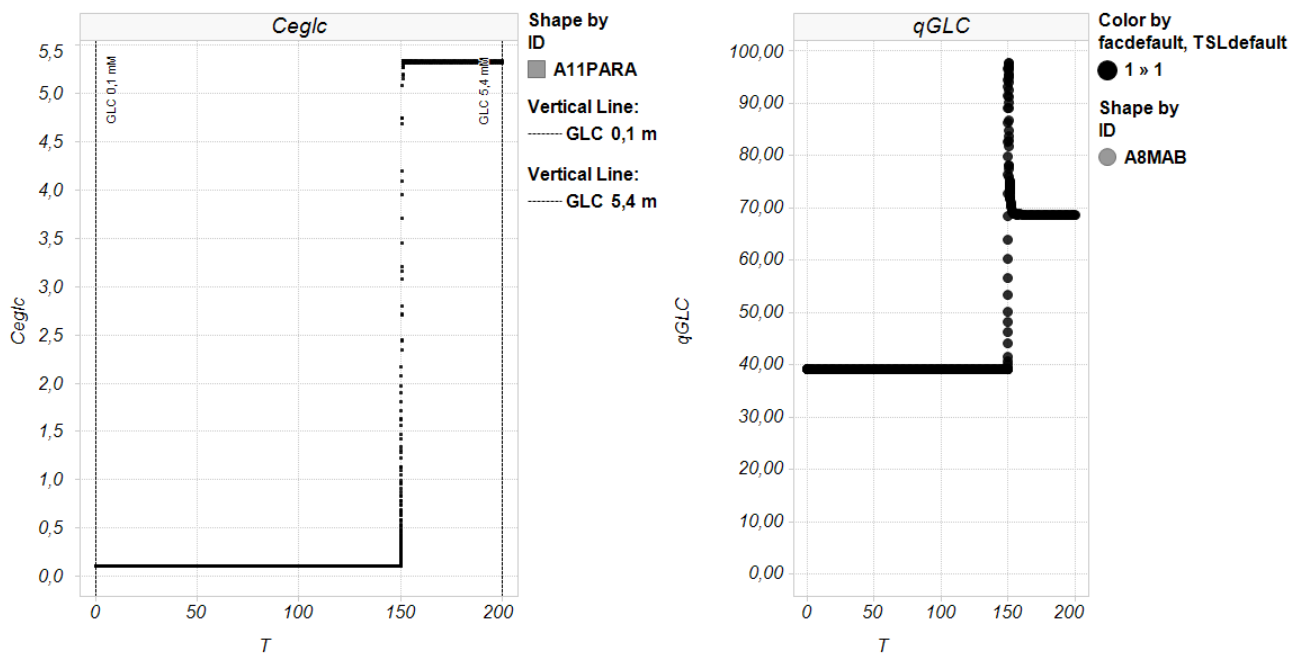


Figure 4: Simple glucose pulse experiment, Glucose concentration in mM and glucose flux in mM/h

The scenario is repeated but this time isozyme ratios and transcript levels of the particular clone are considered. The following graph is used as visual reference about the cell's isoform structure and genetic background.

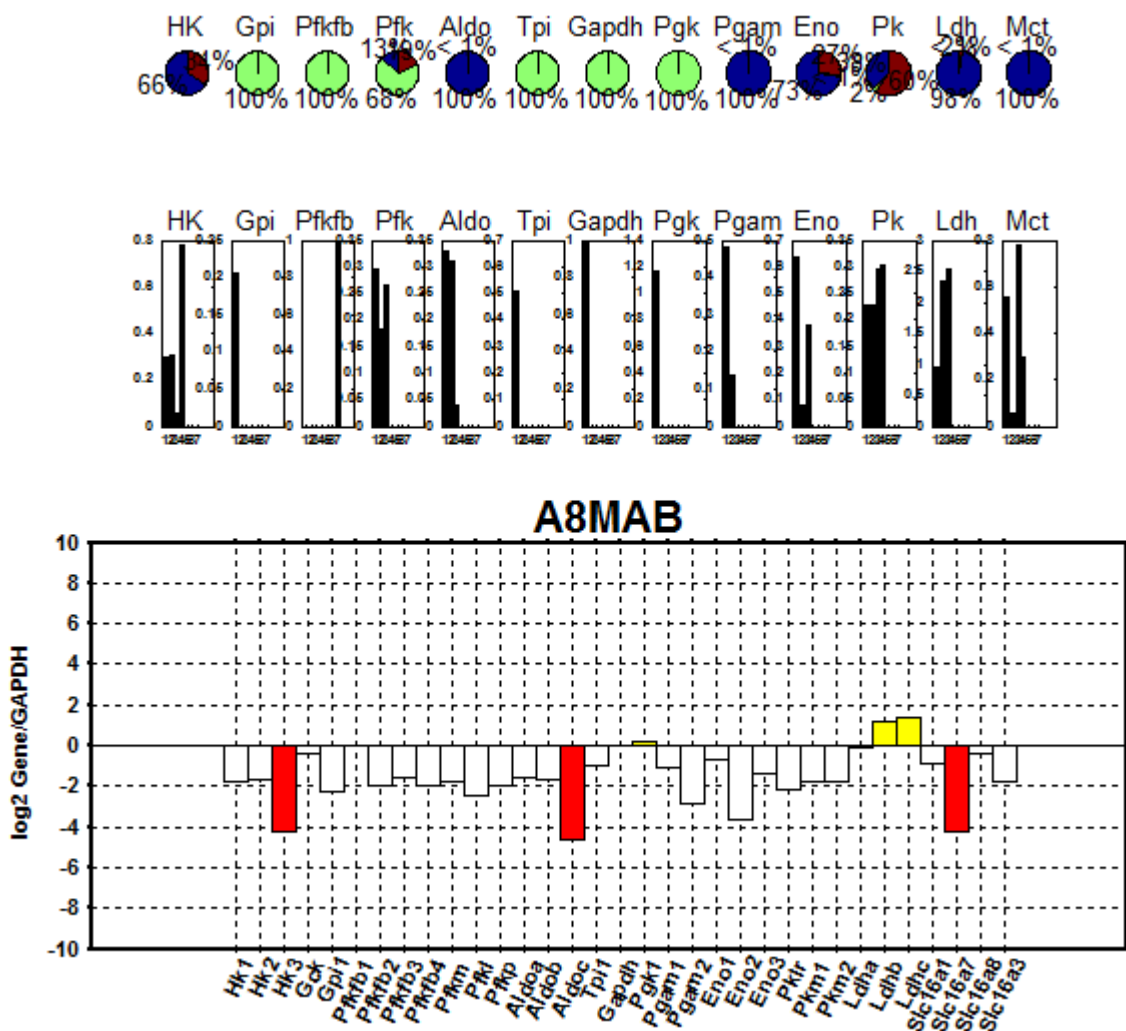


Figure 5: Simple glucose pulse experiment taking the clone's isoform composition into account - Genetic background of clone A8MAB. The bottom bars indicate the biggest three upregulated and smallest three downregulated enzymes, in respect to GAPDH, a housekeeping gene to which transcript levels were scaled.

Indicated as pie are the cell's major isoforms in Matlab's standard colors for categorical data. If only one isoform is available, only one color fills the pie, otherwise more colors are used. The bar charts signify the transcript level (or fold change) of the reaction rate for each isozyme normalized to a housekeeping gene. The y-axis is the numeric fold change and the x-axis the isoform in question in regard to the mean level of this isoform which was determined from all clones. Finally another bar chart represents by which standard the cell line's transcript levels were normalized on log2-scale for a full view of present isozymes compared to the mean and the highest and lowest three genes highlighted in yellow resp. red. A very detailed description of the calculation and a concrete example is given in the appendix and in the formula below. Our contribution does not only include a few selected, but all possible isoforms, their ratio in any given clone, and the amount of transcript readout relative to the mean readout.

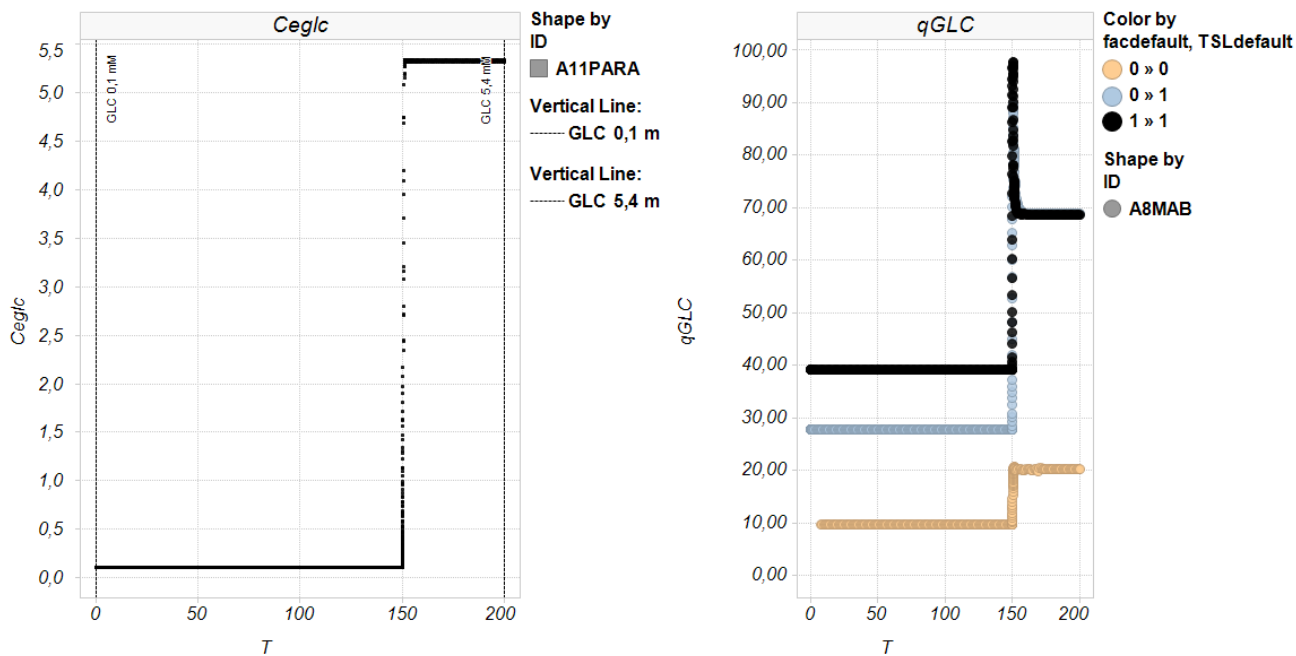


Figure 6: The decision to include isoform composition (blue) or additionally also transcript level (orange) changes the results of the simulations for A8MAB. The default model is black. Glucose in mM, glycolytic flux in mM/h.

The ratio of isozymes is incorporated in the rate equations by modifying the forward reaction with TSL (transcript level), which represents more of the enzyme in question, fractions of the individual rate equations for each isozyme or both. Facdefault 1 represents a default ratio where no isozymes are considered but one dominant form, where the dominant form is the same as in [49]. TSLdefault 1 neglects the effect of increased or decreased enzyme levels and the rate equations are multiplied by a factor of 1. An example of the modified rate equations is given below. Prior experiments were conducted by modifying the isozyme ratio of HK, PFK and PK and transcript levels of PFKFB in a clone, for which the mathematical model was calibrated for [7][11][49].

This contribution considers not only all available isoforms in their exact composition as calculated from the provided transcriptomic data [10], but also the transcriptomic level of any clone in this data sheet. As a consequence, the model may have to be adapted to yield reasonable intracellular concentrations for all clones under investigation. The general form of how transcript levels are incorporated into the existing model is described in the following formula:

$$r_{fw1} = \frac{r_{fw1} \cdot TSL_1 - r_{bw1}}{N_1} \tag{4}$$

$$r_{fw2} = \frac{r_{fw2} \cdot TSL_2 - r_{bw2}}{N_2} \tag{5}$$

$$r = r_{fw1} \cdot Fac_1 + r_{fw2} \cdot Fac_2 \tag{6}$$

The investigated clone A8MAB has a decreased amount of nearly all isozymes and GAPDH, resulting in an absolute decrease of all rate equation modifiers except those for LDHB and LDHC which are increased. Reasons for such low transcript levels may be genetic engineering because of an interest to drive the clone’s metabolism towards a metabolism of reduced lactic acid formation.

Plotting A8MAB versus another clone, A11PARA, under the same conditions yielded very large differences in the genetic architecture of some particular genes responsible for increased glycolytic activity, namely PFKFB3 [64] , PFKL [65], and both HK 1 and 2 [66][67] which have a high affinity to glucose even at low glucose levels.

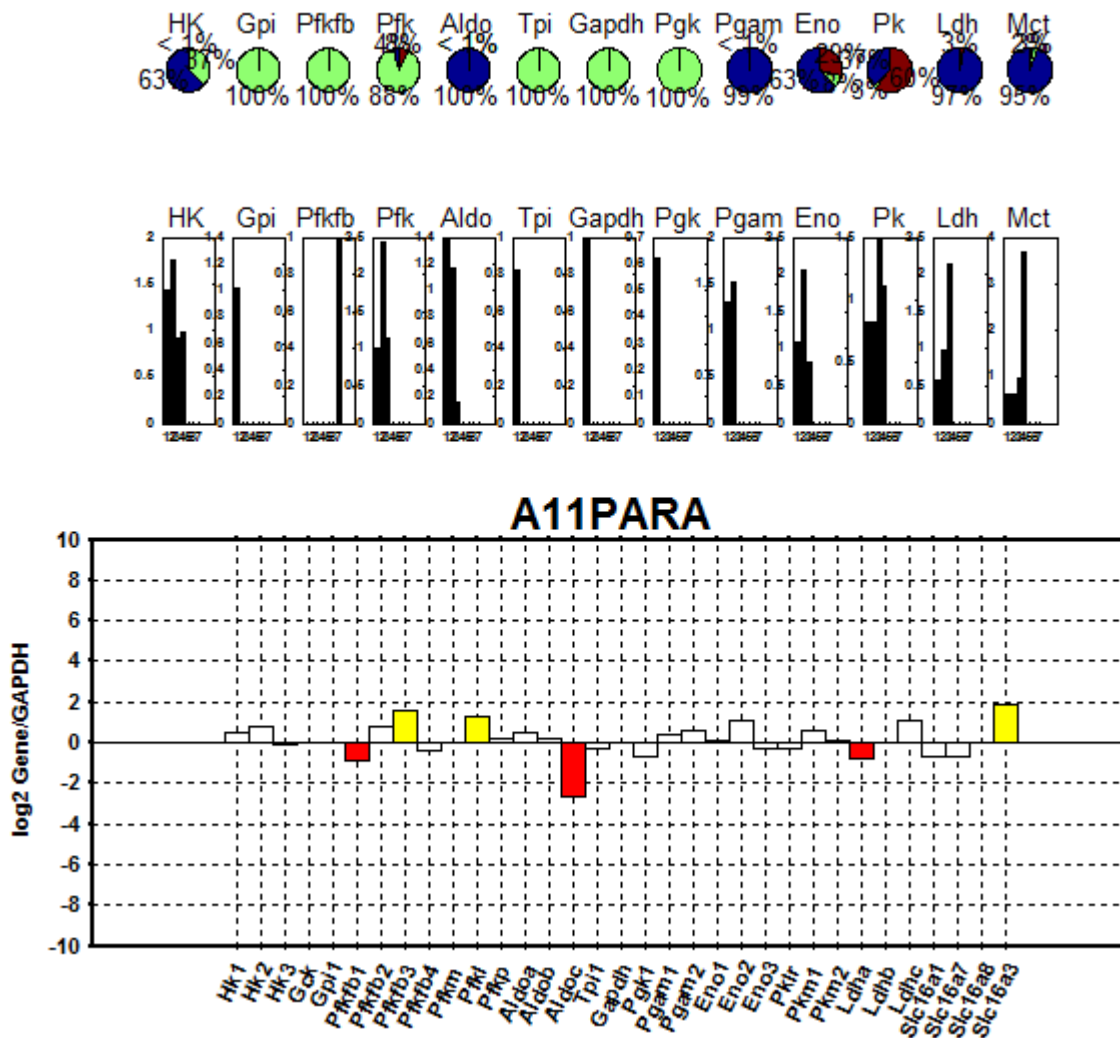


Figure 7: Genetic background of clone A11PARA.

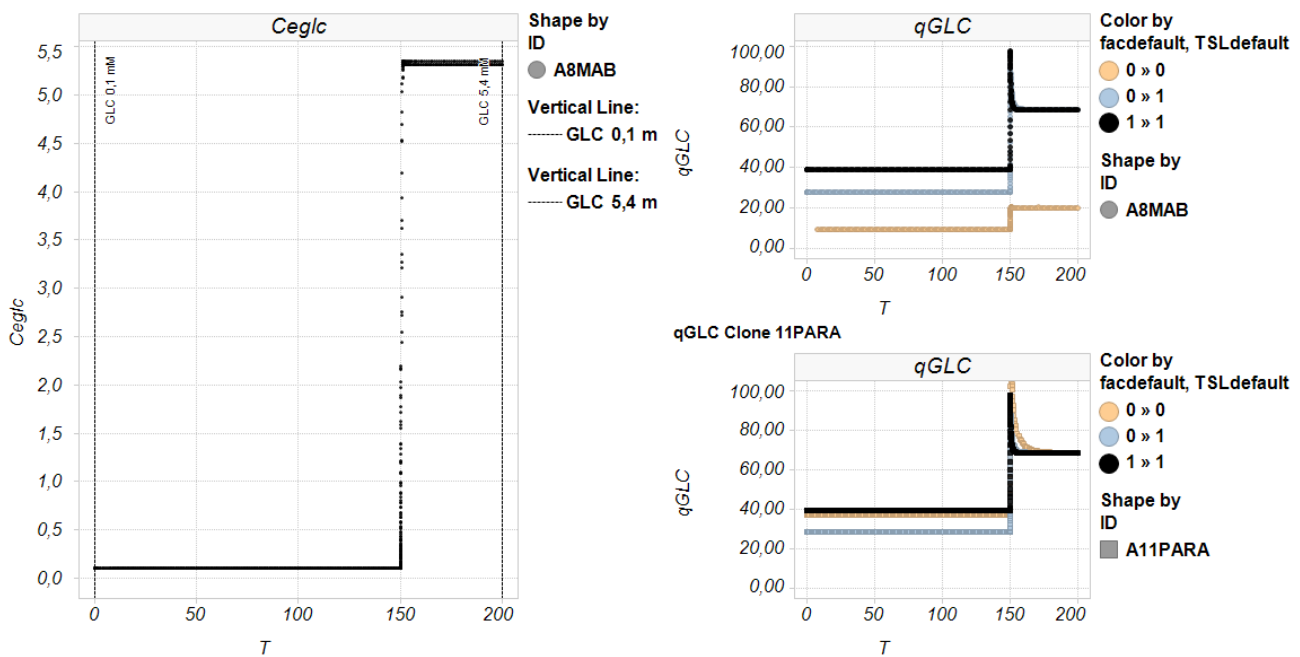


Figure 8: Comparison of metabolic response between two different clones (A8MAB: top, A11PARA: bottom) when isoform composition is taken into account (blue) and when transcript levels are taken into account additionally (orange). The black line represents default behavior. Glucose in mM, glycolytic flux in mM/h.

Simulation results and comparison with the first cell line reveals that glycolytic flux is higher in this clone. They also show that it matters whether only isoform composition or additionally the amount of enzyme according to the measured transcript readouts is considered or not. For further investigations, simulations considering both isoform composition as well as transcript levels were taken into account with the exception of PFKFB3 which stays exactly the same for all clones. The reason for not including changes of this important regulatory enzyme is that an important assumption was made in the early versions of this model and requires more attention.

KbP, an early transcript level-like parameter describing the ratio between forward and backward reaction for the F6P \rightarrow F2,6bP node was set to 10, and acting on this value with two more factors could lead to a situation where more F2,6bP is consumed than is available because the backward reaction rate becomes larger than the forward rate even when F2,6bP is already zero. This problem arises because KbP must be known, at least approximately. It can assume values between 0,4-710 [49] between tissues and clones. An excel sheet is provided to better explain the problem. However, if the exact KbP is known or well estimated, it can be set individually to the desired value and a change of PFKFB3 can be simulated for any individual cell line instead of making this assumption for all clones.

Conclusively, as a first step, transcriptomic information was integrated into the mathematical model under the following considerations:

- The original model without implementing isoform composition or process events can be used to test metabolic response to a different chemical environment
- By introducing isoform ratios, metabolic changes between all clones can be observed, i.e. under glucose limited conditions. However, isoform composition can potentially be very similar and result in almost no difference between clones in the simulation.
- Transcript levels of enzymes may yield more interesting results since some clones have more of the same isoform than others. This quantity is difficult to represent for two reasons: first, a higher transcript readout does not automatically mean a higher enzyme concentration and vice versa. On the other hand, not including such an important effector of rate speed may lead to oversimplification of otherwise very different transcript levels between clones.
- Calibration – some assumptions may need revision, such as the transcript level and basal reaction rate of PFKFB3 or other enzymes, which are modified by both a transcript level and isoform composition factor. If clones should be tested under the same standardized conditions, concentrations of any intermediates may not turn negative or reach unphysiological concentrations in the simulations.

We have shown that the way to analyze transcriptomic integration into a mathematical model may affect the results of the simulations. We decided to use both isoform composition and transcript levels in further simulations to reflect both effects in distinct scenarios as accurate as possible.

3.3. Influence of pH shift

The basic model involves a transporter equation for lactic acid which explains how chemical equilibrium between cytosolic pH and cytosolic lactic acid and extracellular pH and extracellular lactic acid can drive lactic acid production or consumption. To show the mechanism in action, a pH shift was simulated for both clones and its impact on the lactic acid profile and viable cell concentration shown. To gain the most insights from the experiment, the experiment shows cell metabolism i) at a low glucose concentration and high pH, ii) at a high glucose concentration but low pH, and iii) at a high glucose concentration and high pH.

While in the simulations both cell lines start alike, their behavior during a pH shift diverges due to a difference in genetic composition. After the first pH shift by -0,2 units, lactic acid production is reduced for both clones. But while clone A11PARA continues producing lactic acid, A8MAB begins consumption. After glucose is restored to a higher level, lactic acid production sets in again due to an increase in glycolytic flux, albeit with different specific production rates. A final pH shift back in the same order of magnitude leads to increased lactic acid production once more.

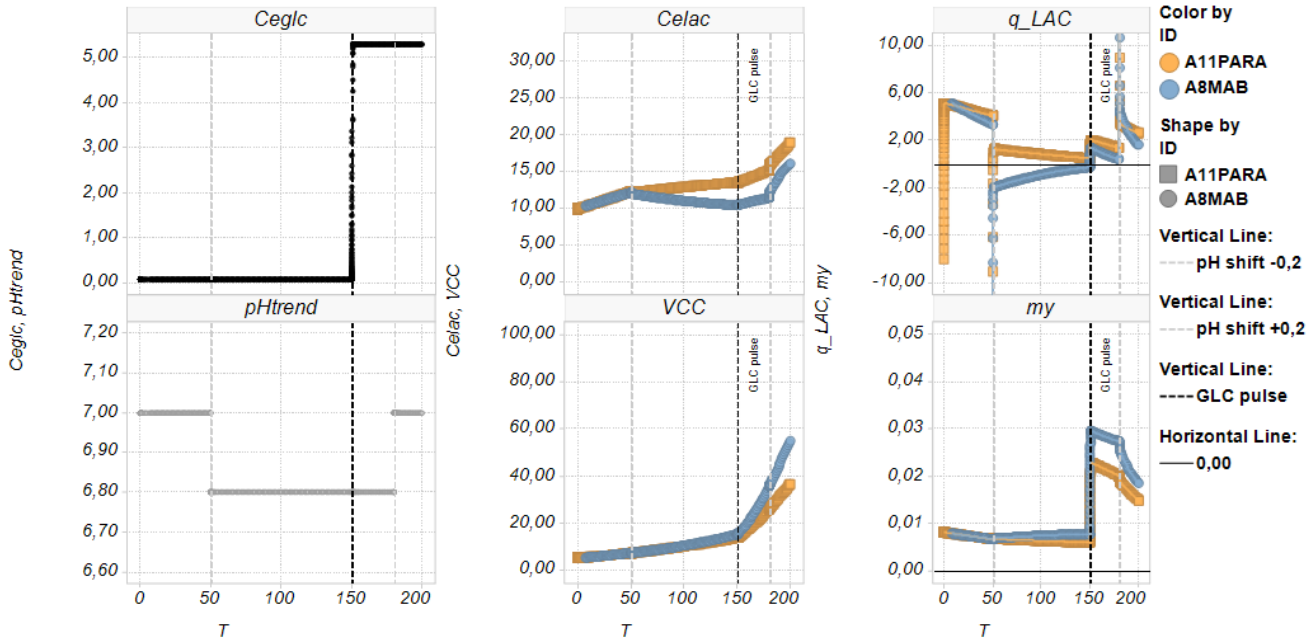


Figure 9: Influence of pH shift. Two clones are compared in their metabolic response of pH shift: A8MAB (blue) and A11PARA (orange). External glucose and lactic acid concentration in mM, VCC in E5 cells/mL, lactic acid flux in mM/h, growth rate in h-1.

The simulation results indicate that A11PARA may be a stronger consumer of substrate and stronger producer of metabolites in the form of lactic acid, whereas A8MAB might consume less substrate but finally be less inhibited by lactic acid as seen in the total number of viable cells at the end of the simulation.

Growth is explained by the standard model using the following relationship between glucose availability and lactic acid inhibition, which was used in a continuous culture experiment [7] but may have to be modified to better fit the scenario's reality.

$$\mu_{standard} = 0.055 \frac{C_{GLC}}{C_{GLC} + 0,3} \cdot \frac{144}{C_{LAC}^2 + 144} \quad (7)$$

A pH shift may lead to a reduction in lactic acid production, but it may have also other less desirable effects, such as reduced cell growth. An external pH may shift the internal pH by a few units depending slightly on cell clone [36], which then may act directly on the cell's rate limiting enzymes in glycolysis, such as HK [42][68] and PFK [69][70].

3.4. Influence of pHe on pHi

How much the external pH correlates with internal pH can be assessed by one-time calibration. However, this is somewhat problematic for a screening tool with different cell lines, because finally, the calibration curve may vary slightly between clones. Still, we believe that assuming a constant pH gradient during pH shifts is farther from reality than using an experimental reference conducted with mammalian cells and therefore enable this reversible option for our model simulations. Allemain et al. have measured exactly this relationship in fibroblasts and found that different clones have a relatively constant slope.

An increase of roughly 0,55-0,6 units pHi per 1 unit increase in pHe [36] can give an estimate how much other cell lines might differ from each other. The slope is relatively constant, but the intercept may be different. Since we are interested mainly in the slope, which is the relationship between pHi and pHe, we find this less problematic for our purpose. Therefore, even though clone to clone variance is possible, this relationship may hold fairly true for most simulations and therefore be used to investigate how metabolism can change over time. The relevance of this finding may help modeling cells even more accurately in a pH-dependent manner and is explained in more detail below.

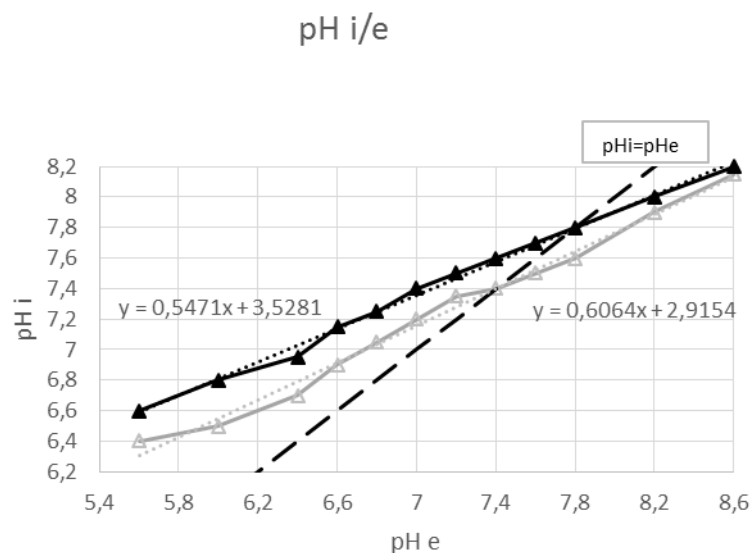


Figure 10: Relationship between pHi and pHe as published by Allemain [36]. The data was used to calculate slope and intercept. Two different fibroblasts were compared in culture, one paternal line (black) and a mutant lacking Na⁺/H⁺ exchange (white). For our purposes, the slope from the wild type (black) was considered.

The question is how pH change could be used to alter the rate in our glycolysis model. Mulquiney [44] modeled the impact on the forward reaction of HK by a bell function,

$$pH \text{ factor} = \frac{1}{1 + \frac{10^{-pH}}{10^{-pK1}} + \frac{10^{-pK2}}{10^{-pH}}} \quad (8)$$

where pK1 is 7,02 and pK2 9,0. At pH 7,3, the fold increase factor is 0,65. Because the maximum flux in the bell function is around pH 8, but the model flux used pHi 7,3, normalization was required. Changing pH between 6,6 and 8,0 now corresponds to a change in glycolytic flux by a factor between 0,58 – 1,3.

Comparison with literature, where the impact of external pH on glycolytic flux was investigated [39] reveals that a flux change is reasonable as the glycolytic rate in experiments decreased to little more than a third of its typical rate in case of a pHe shift from 7,2 to 6,8 and increased after pHe shift from 7,2 to 7,8 by more than two-fold. However, these experiments were conducted in the first two days of a batch culture, where specific glucose uptake is subject to very large changes. Our calculated “squeeze” of glycolytic flux rate is rather conservative in comparison by assuming that a pHe change of 0,2 units would not increase the glycolytic flux by more than 0,1 pHi units. However, often batch or even fed-batch cultures start at a much higher pH because of the anticipated lactic acid formation, thus a total pH change from 7,4 to 6,8 is possible which is in the experimentally observed flux change range.

Conclusively, this adds an aspect to the simulation without exaggerating its effects in the range pHi 6,6 – 8 which corresponds to a pHe of 5,6-8,2 as depicted in the pHi/pHe relationship above with pHi of 7,3 as norm. As pHi does not change massively, but slightly, we hope to point out how cultivations at different pH or long-time pH shifts may lead to a different metabolic profile of the culture, especially if the explored difference in pH is very large and must be taken into account.

Table 1. Relationship between pHi and glycolytic flux. At pHi 7,3 there is no effect on glycolytic flux

<i>pHi</i>	<i>final pH factor influencing flux</i>
6,6	0,42
6,8	0,58
6,9	0,66
7	0,75
7,1	0,84
7,2	0,92
7,3	0,99
7,4	1,07
7,5	1,13
7,6	1,18
7,8	1,26
8	1,28

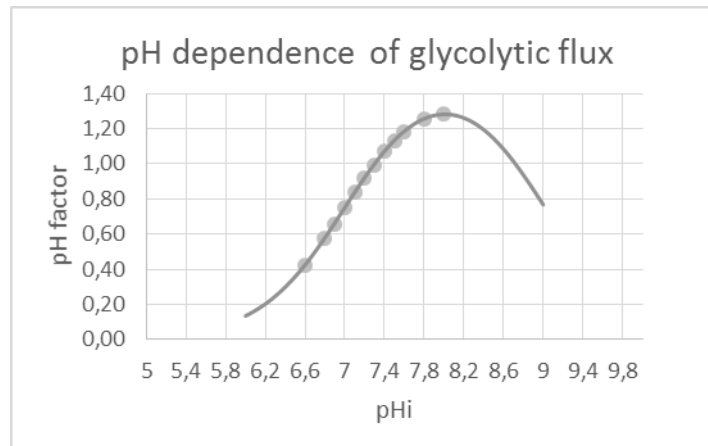


Figure 11: Relationship between pHi and glycolytic flux in modeled erythrocytes. The pH factor is a dimensionless multiplier of the forward reaction of pH sensitive enzymes, such as HK or PFK [39].

The pH factor as presented by Mulquiney's bell-curved relationship [39] between metabolic flux and pHi was used to multiply the forward rates of HK and PFK, the rate-limiting steps in glycolysis, by assuming that pHi has the same effect on both two enzymes. Finally, a decrease in glycolytic flux is considered to influence growth rate negatively and is represented in form of the following modified growth equation of the original model:

$$\mu_{custom} = 0.055 \cdot pHfactor \cdot \frac{C_{GLC}}{C_{GLC} + 0,3} \cdot \frac{144}{C_{LAC}^2 + 144} + death\ constant \quad (9)$$

At least one term in the growth equation should consider a decrease in cell growth to better reflect fed-batch behavior in which cell viability decreases over time. It may depend on many other factors than the linear functions with which it is represented and is set to zero in these simulations but may be used in fed-batch simulations where cell concentrations decrease after some days of cultivation.

The additional coefficients pH factor can be used if pH or excessive lactic acid is believed to have an effect on the specific growth rate which could result in slower growth as experienced in practice. Osman et al. have probed the growth behavior of cell culture after pH shifts in a wide range between 6,5 and 9, and came to the conclusion that cells grow best between pH 7,3-7,5 and antibody productivity was highest around pH 7,1 [71]. Several reasons for an increase in glycolytic flux at higher pH were proposed, including an alteration in membrane potential which facilitates glucose import, more lactic acid production to counter alkaline pHe to maintain pHi [72]. If for the current problem statement pH is controlled perfectly, or for other reasons have no effect on growth, the standard growth equation (7) can still be used instead. For our following next simulations, pH was considered.

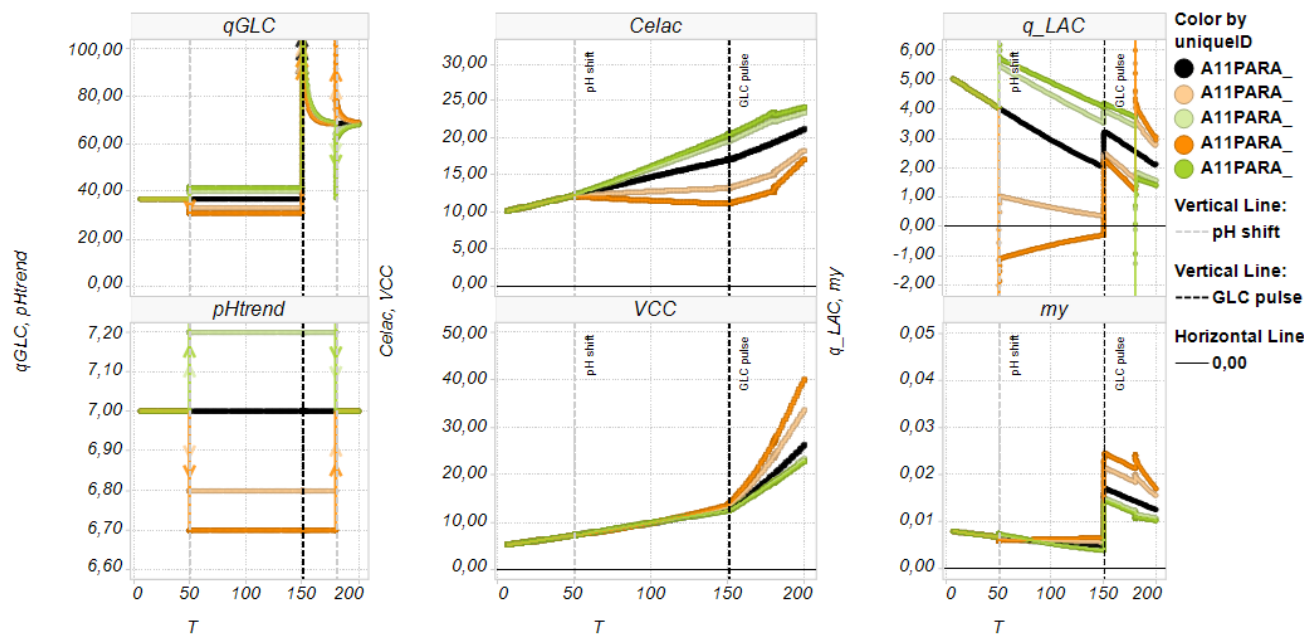


Figure 12: Effect of pH shifts of different intensity (shade) and direction (green: + 0,2 or + 0,3 units, orange: -0,2 or -0,3 units). Lactic acid in mM, VCC in E5 cells/mL, glycolytic and lactic acid flux in mM/h, growth rate in h⁻¹. Shift in pH and glucose concentration (from 0,1mM to 5,3 mM) is added as grey and black dashed lines on all plots.

The simulations show that an acidic pH shift reduces the specific glucose and growth rate slightly (from pH 7 to 6,8), which does not have a big impact in limitation, except that lactic acid levels are kept low due to the reduced lactic acid production rate, which, depending on the intensity of the pH shift, can turn to lactic acid consumption. Comparing these simulations results to literature, Kurano et al. observed a decrease of growth rate, specific glucose uptake rate and specific lactic acid production rate as an effect of pH [73], where growth peaked at a pH of 7,6. Osman et al. [71] produced similar results in fed batch culture, where he observed peak cell growth at pH 7,3-7,5 but peak volumetric antibody production at pH 7, indicating a strong link to metabolic efficiency.

Our results indicate that the major process technological advantage of this cultivation strategy may lie in the ability to keep viability high in the form of an initially lower, but constant growth rate [74]. Upon glucose pulse, all specific glucose uptake rates approach their physiological maximum because the enzymes work at their full capacity. A pH shift back to norm conditions perturbs the equilibrium between inner and outer lactic acid and H⁺ concentration once more and leads to adaptation of the specific lactic acid production rate.

We wish to remind the reader that this is a scenario in which the cell line in question is tested for its individual metabolic response. By providing a simulation including both a pH shift down and shift up at two distinct glucose concentrations, we are able to make a statement about metabolism in both limited

and non-limited process conditions. The results could then be used as guidance whether the clone would be suitable under limited conditions or not and how much a shift in pH might affect cells in a limited or non-limited environment in order to find the most efficient metabolic behavior.

3.5. Timing and intensity of pH shift

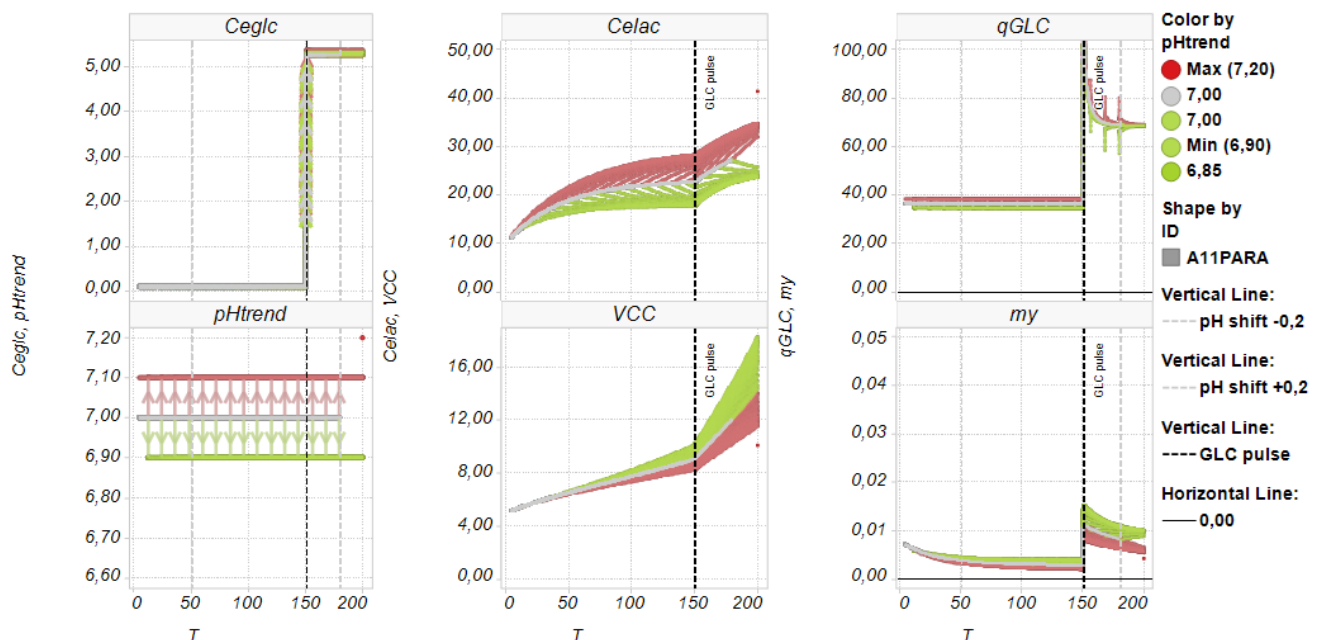


Figure 13: Effect of different timing of pH shifts of different direction (green: pH shift - 0,1 units, red: pH shift + 0,1 units). Only one pH shift was performed per simulation, the time window for pH shift exploration was 12h and all results are plotted in one window. Glucose and lactic acid in mM, VCC in E5 cells/mL, glycolytic flux in mM/h, growth rate in h-1. Shift of glucose concentration is added as dashed line on all plots.

Simulations show an effect in the timing and intensity of pH shifts, which can be as important as the decision how to hold a particular glucose concentration. The scenario was set to simulate a unique pH shift of 0,1 after 12h, and the scenario was repeated by delaying the pH shift another 12h without returning to the initial pH, but a glucose pulse at the end to determine the effect of non-limited behavior after some time of incubation in limited glucose conditions. As a result, every scenario has one shift in its runtime, the direction of the shift is distinguished by color (green: shift down 0,1 pH units, red: shift up 0,1 pH units), and all of them are plotted together above.

A small shift of only 0,1 pH units resulted in a transient lactic acid difference which caused the growth rate to differ by as much as 50% upon glucose shift just because of reduced lactic acid concentration. Such a scenario, with a less severe limitation as in this example, could become relevant during seed train

expansion where cells are transferred into fresh medium and experience a sudden growth impulse after each stage and where the optimal timing between transfers would be of interest to modification.

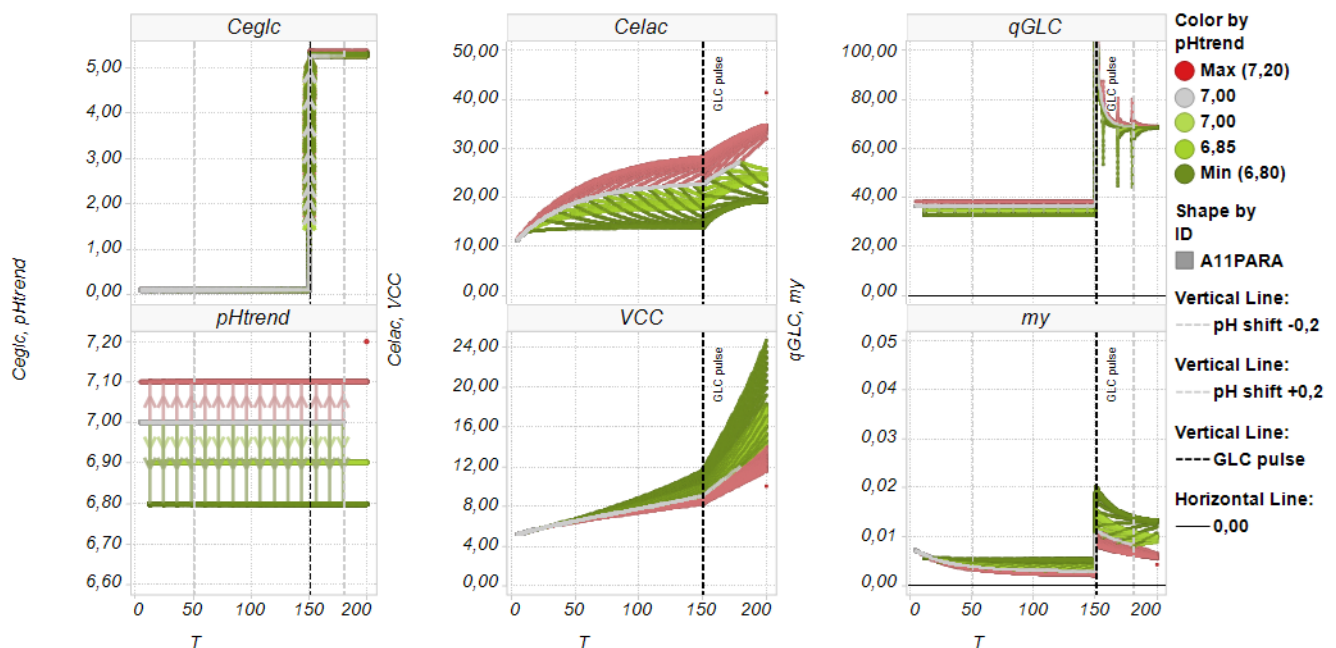


Figure 14: Effect of different timing of pH shifts of different direction and intensity (green: pH shift - 0,1 and - 0,2 units, red: +0,1 units). Only one pH shift was performed per simulation, the time window for pH shift exploration was 12h. Glucose and lactic acid in mM, VCC in E5 cells/mL, glycolytic flux in mM/h, growth rate in h-1. Shift of glucose concentration is added as dashed line on all plots.

The shift experiment was repeated for -0,2 units in pH and differences in the speed at which lactic acid was consumed could be observed. The later the pH shift happened, the more lactic acid was already present in the extracellular environment and the more cells could use the larger gradient to increase their lactic acid consumption rate as described in literature [75]. Comparison between 4 pH ranges indicates that although both glycolytic rate and growth rate is slightly reduced at lower pH, the growth rate benefits more from the reduction in lactic acid than it suffers under a pH shift and assumes up to two fold larger values after the glucose pulse than cells which were cultivated at a higher pH and have a larger lactic acid inhibition by then.

A pulse-wise dosage of glucose results in glucose concentrations in a range way above the physiological level does not only harbor the risk of glucose starvation as a result of manual feeding, i.e. when operators make a mistake in administering glucose or add it too late or at a too low dosage [76], but the metabolic profile is expected to be more growth-inhibiting due to lactic acid accumulation compared to a continuous, ‘feed what you need’ strategy.

Such a continuous feeding strategy is possible only with appropriate online-capable equipment such as off-gas analysis [77][78][79], capacitance probe [80][81][82] or combinations of those and other methods [60], [83]–[86] and often glucose concentration comes close to the K_m range of glucose transporters [87]. Such a mode of operation may be not only beneficial in terms of keeping viability higher [88] than in a standard process, but also improve the stability of the chemical environment (external glucose and lactic acid concentrations), which may stabilize pH control [89] and reduce process events, and finally lead to a higher titer [90], better product quality [25][91] or a synergetic mixture of all.

The point in not using i.e. a black-box model is, that different cells react differently to process control strategies, but especially so under glucose limiting conditions. Most mammalian production cell lines are difficult to describe mechanistically when the culture operates always way above the physiological range in a non-limited environment because often the resulting parameters may change when the model is tested on other clones. Our approach is to describe growth mechanistically under conditions where real enzyme parameters are used in rate equations and a different composition of isoforms has an impact on metabolic flux. For instance, glucose influx can be described as a function of glucose concentration, and depending on which isoform composition is available in the clone and how much is present, the resulting rate will differ greatly among clones and some examples will be provided in the next section to explain this in detail.

3.6. Explorative Protein engineering

This model has fully explorative kinetic parameters which can be changed any time to better understand the system. To do this, the provided excel sheet can be used to change i.e. affinities to substrate. By getting to know the regulations first-handed in simple and short simulations, parameters may be also changed to see their impact on the process scenario result.

The following parameters were changed to simulate how a modulation of isoform could have a different outcome in the simulation. Differences in isoform behavior (terms in rate equations) and kinetic properties (numeric parameters such as substrate affinity) are not fully explored for all isoforms yet. For instance, there are 4 isoforms for LDH, but often important information is missing, such as the exact composition of the tetramer fraction of the isozyme. These tetramers can then i.e. influence the parameter for product inhibition, and affect lactic acid behavior of the clone [92]. In lieu of concrete isoform data, the following approximations may be as informative instead: a ten-fold increase of an available “norm”, which is determined from literature usually not considering isoforms, is increased or decreased to simulate how LDH isoforms having those fold changes in important parameters would change metabolism. The parameters which were modified were the K_m for pyruvate and LDH enzyme level.

Table 2. Possible targets for enzyme modifications

Enzyme	Target	Color code	Black	Blue	Green
LDH	Km Pyruvate	Current norm (0,2mM)	0,02mM	0,02mM	2mM
LDH	Enzyme level	Current norm (0,00343)	0,000343 (10-fold decrease)	0,000343 (10-fold decrease)	0,0343 (10-fold increase)
HK	Km Glucose	Mixture depends on selected clone	0,001mM	0,001mM	0,1mM
HK	Enzyme level	Current norm (0,047)	(0,0047) (10-fold decrease)	(0,0047) (10-fold decrease)	(0,47) (10-fold increase)
PK	Km F1,6bP	Mixture depends on selected clone	0,01 mM	0,01 mM	1000 mM (virtually no binding to activator)
PFK	Enzyme level	Current norm (0,0002)	0,00002 (10-fold decrease)	0,00002 (10-fold decrease)	0,002 (10-fold increase)

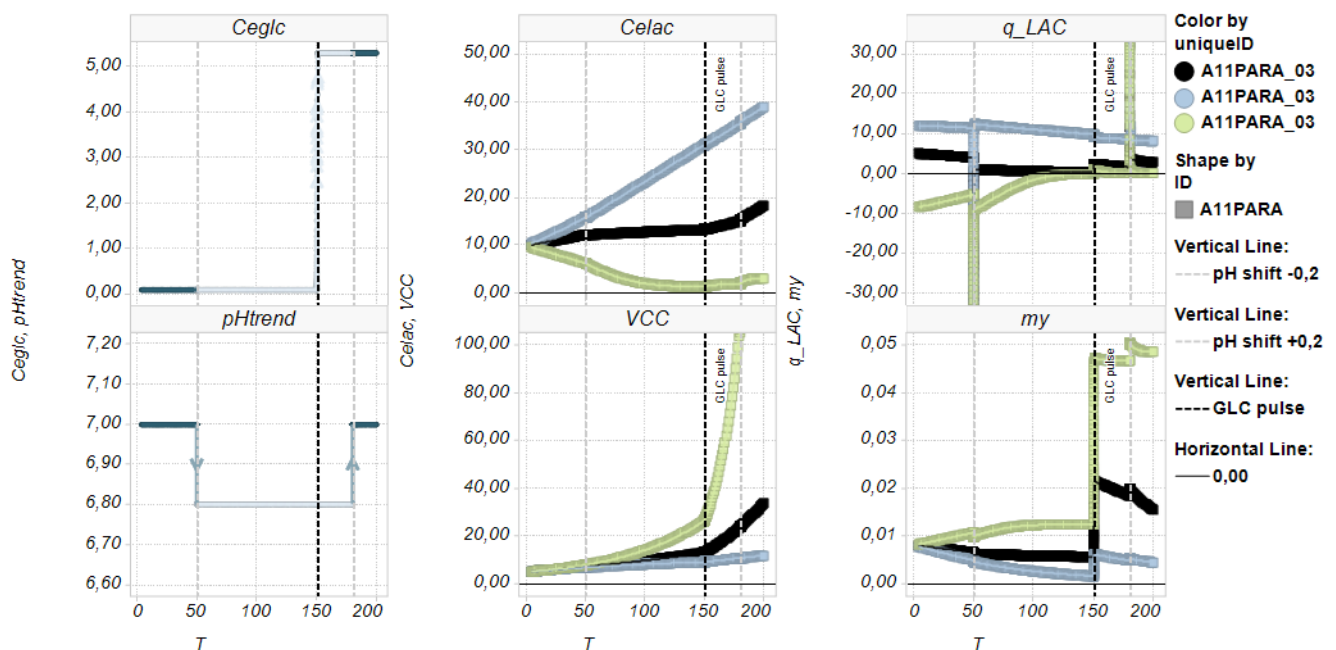


Figure 15: Effect of changed kinetic parameters in LDH: substrate specificity. Glucose and lactic acid in mM, VCC in E5 cells/mL, lactic acid flux in mM/h, growth rate in h-1. Shift of pH and glucose concentration is added as grey and black dashed lines on all plots.

Upon a change in Km of LDH to pyruvate by a factor of 10, lactic acid consumption behavior was markedly affected. A tenfold increase in Km of pyruvate resulted in immediate lactic acid consumption which not even a bolus shift or pH shifts could noticeably affect. As a result, our modeled growth rate

was at first limited, while glucose was limited, but after the pulse shifted to its maximum value as no inhibitory external lactic acid was present at all. On the contrary, decreasing K_m of pyruvate tenfold resulted in a constant lactic acid production.

Conclusively, protein engineering of LDH may result in low lactic acid levels in newly engineered clones which may have a more efficient metabolism and be easier to cultivate in culture because they would by themselves not produce as much lactic acid as the paternal line. However, in practice this could also mean that their ability to grow might be impaired. This is why it is important to understand which parameters influence metabolite formation and which influence growth. By setting up for instance a much higher pH, a low growth rate might be increased and the clone would potentially still have a low lactic acid production rate.

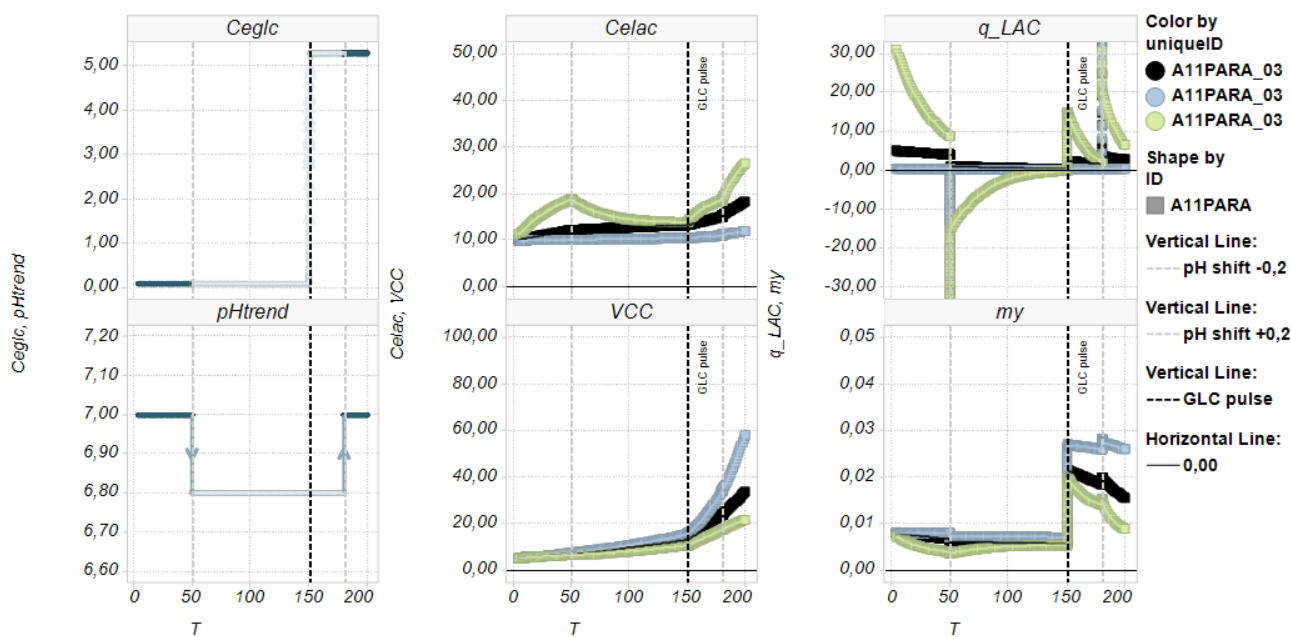


Figure 16: Effect of changed kinetic parameters in LDH: enzyme transcript level. Glucose and lactic acid in mM, VCC in E5 cells/mL, lactic acid flux in mM/h, growth rate in h⁻¹. Shift of pH and glucose concentration is added as grey and black dashed lines on all plots.

Modifying the transcript level of LDH has also a direct metabolic effect. With more LDH, lactic acid production and consumption are both stronger pronounced in the given process conditions, while with less LDH it takes longer to reach equilibrium.

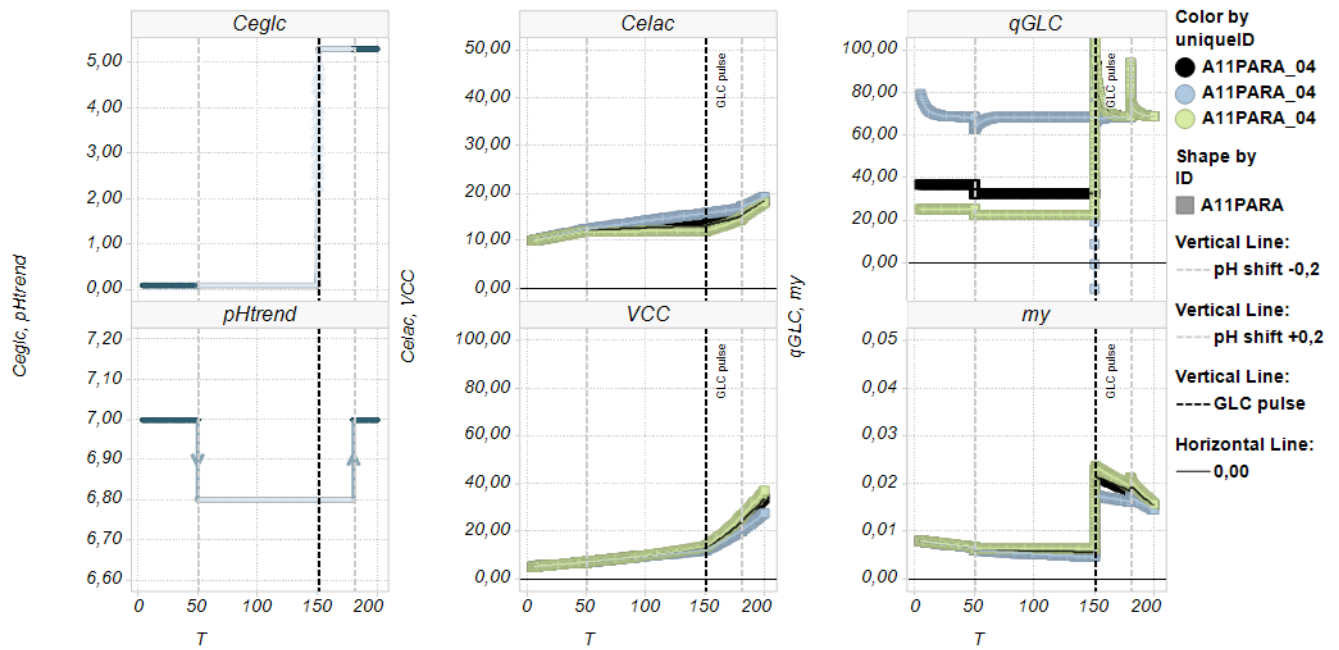


Figure 17: Simulation of pure isoforms in HK. Black: default clone, blue: Km glucose artificially set to 0,001mM (closest to HK III isoform), green: Km glucose artificially set to 0,1 mM (closest to HK I isoform).

Applying the same artificial changes to HK results in an interesting artifact which is based on the simulation scenario: increasing specificity towards substrate (low Km, blue) results in maximum glycolytic flux, but low lactic acid production rate because of flux channeling to the TCA. The growth rate meanwhile is rather low because the model's growth is described by glucose concentration and lactic acid inhibition, but not glycolytic flux itself. The flux, but not growth rate of the lowest substrate specificity to glucose (high Km, green) is lowest in this experiment. All fluxes rise when sufficient levels of glucose are available again, because the concentration is far above Km in this scenario.

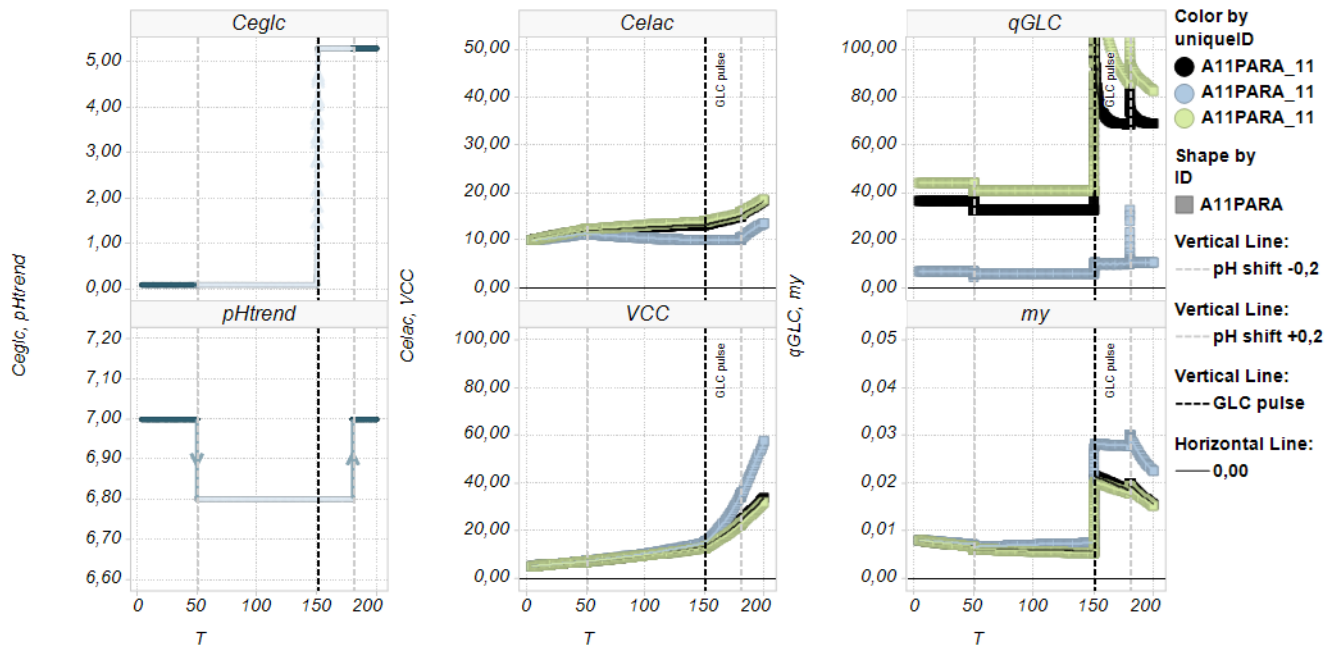


Figure 18: Simulation of different enzyme levels in HK. Black: default clone, blue: enzyme level of standard model artificially decreased ten-fold, green: enzyme level of standard model artificially increased ten-fold.

Changing (all) HK enzyme levels artificially by ten-fold reveals that the isoforms have an impact on glycolytic behavior, because more enzyme will not change flux dramatically, if substrate specificity is as low as in the default model. But if enzyme levels are decreased ten-fold, glycolytic flux is decreased. This makes sense because few available catalysts are not enough to sustain a high flux, even though the chemical environment would allow it with the given specificity of the catalyst. This becomes even more apparent when glucose is shifted up, and the flux is barely increased. Conversely, viable cell count would be highest in this simulation, simply because a high concentration of glucose and low concentration of lactic acid would lead to a very high calculated growth rate with the given formula.

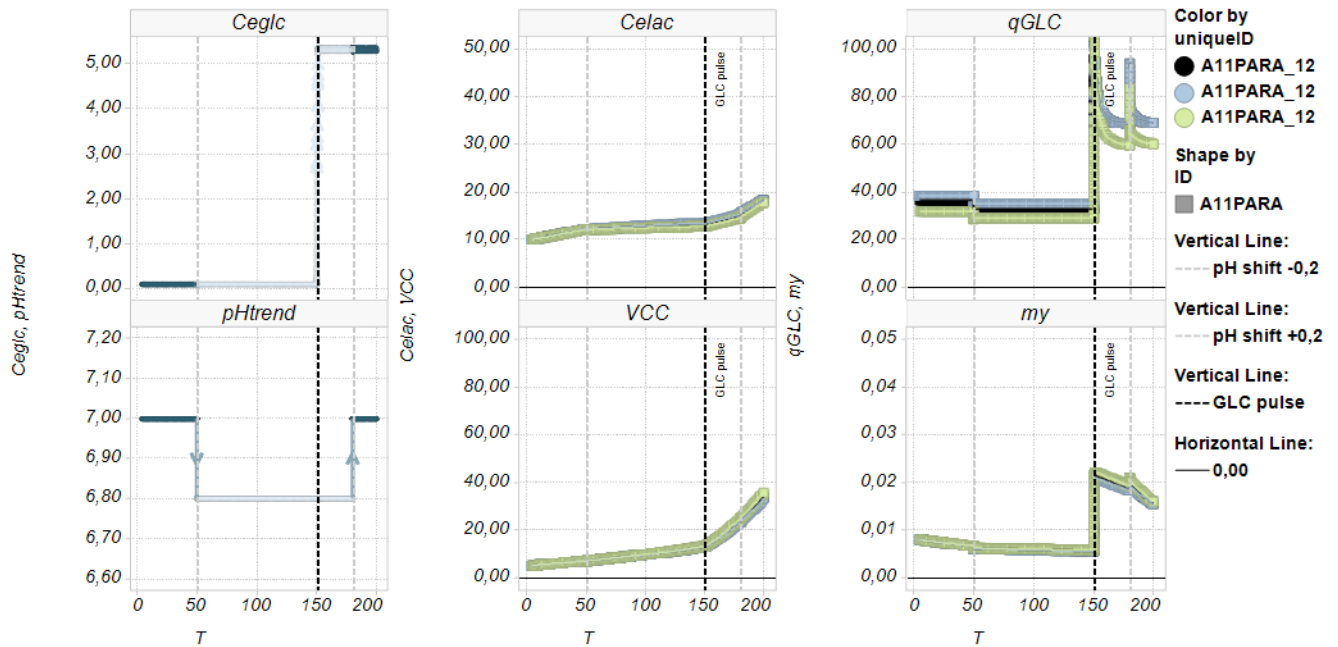


Figure 19: Simulation of binding to an activator in PK. Black: default clone, blue: high specificity to activator F1,6bP (PK-L type, Km 0,01), green: low specificity to activator (PK-M1 type, Km 1000).

Changing Km F1,6bP of PK to high substrate affinity (low Km, blue) results in a slight increase in flux with respect to the default behavior. Upon changing glucose concentration, the already strong affinity does not influence the flux any further, but it can be seen that a lower substrate affinity of the glycolysis activator F1,6bP leads to a reduced glycolytic flux by ca. 10% (69 versus 60 mM/h) which indicates that the reduction of substrate affinity can be used to direct cells metabolism to “get stuck”, or rate-limited, at different stations of glycolysis, depending on allosteric regulation of the other intracellular metabolites. This involves the concentration of the activating or repressing substrate.

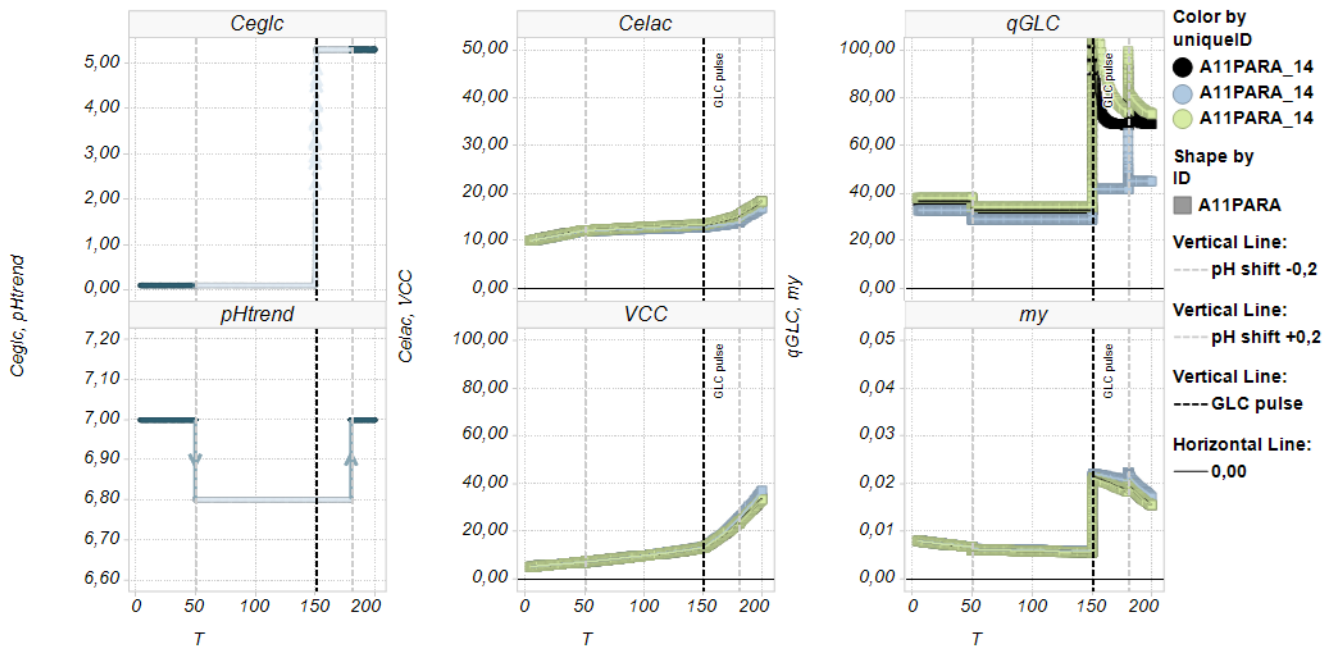


Figure 20: Simulation increased enzyme level in PFK. Black: default clone, blue: low (10-fold decreased) concentration of PFK leading to low levels of F1,6bP, green: high (10-fold more than default) concentration of PFK leading to low levels of F1,6bP. In the extracellular rates and concentrations, differences are noticed only in reduced glycolytic flux when PFK is reduced.

In our simulations, many assumptions from a calibrated model were passed on into this model, which is in its current form designed to simulate metabolic behavior in different cell lines. By doing so, several intermediate concentrations are out of their original bounds because parameters which were fitted to one clone may not fit to all the other clones any longer [44][93][94][95][96][97]. One very important intermediate which may require adaptation to physiological concentrations is F1,6bP.

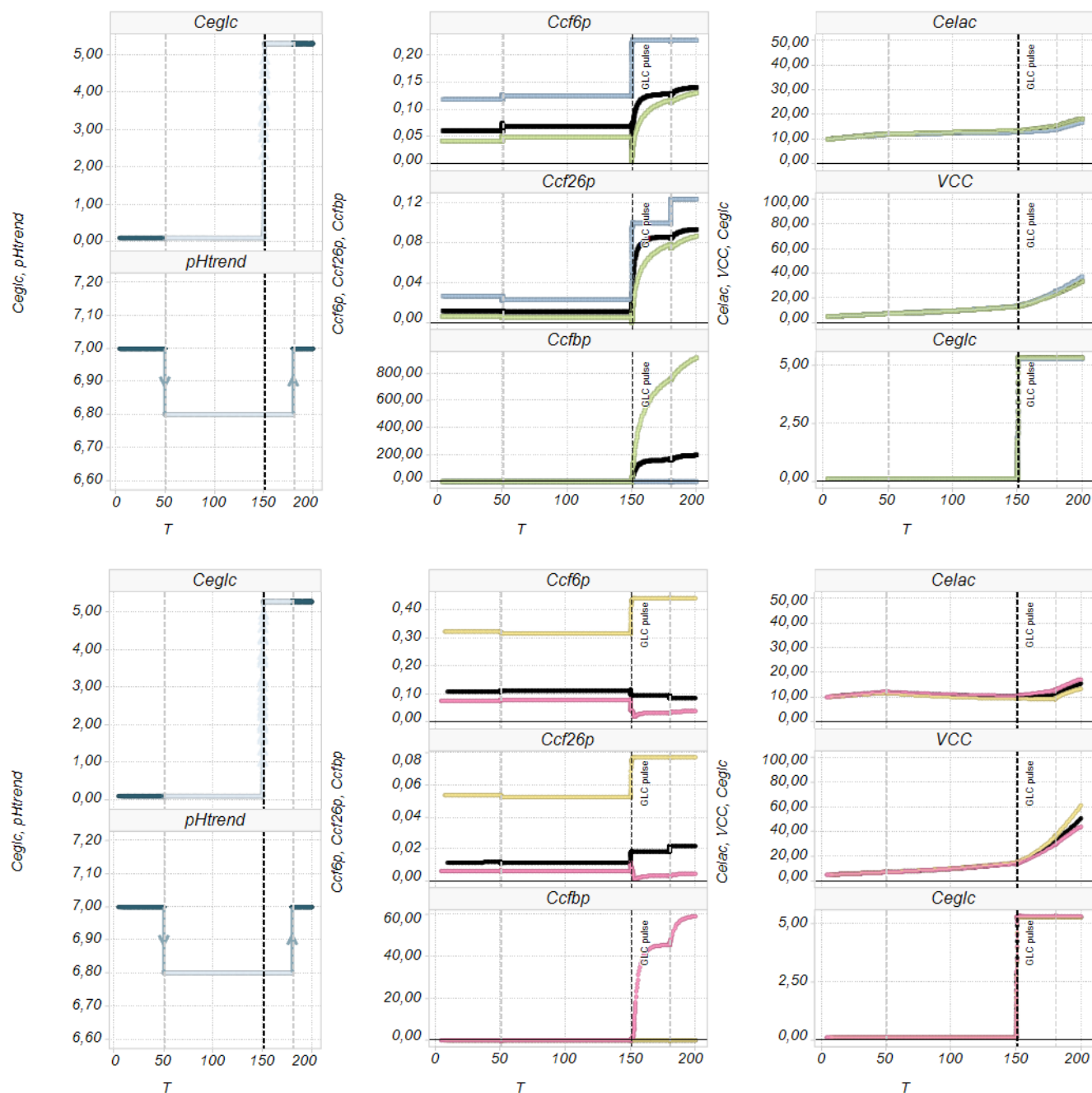


Figure 21: Sensitivity of the PFK node to parameter modification. Black: default clone behavior 11PARA/8MAB, blue/yellow: low (10-fold decreased) concentration of PFK enzyme level, Clone 11PARA/8MAB, green/pink: high (10-fold more than default) concentration of PFK enzyme level, Clone 11PARA/8MAB. Concentrations from top to bottom: F1,6bP, F2,6bP, F6P, lactic acid and glucose in mM, VCC in E5 cells/mL

The problem of a necessary parameter fit can be rarely seen in extracellular rates or concentrations alone, but rather in intracellular accumulations of metabolites in concentrations beyond natural limits. These occur when very sensitive reactions are modified with multipliers like isoform composition or transcript levels as was the case here. For allosteric regulation it does not matter much whether the concentration

is 10 or 100 mM, when the activation occurs at values over 1mM to 100% already. But it does matter when the chemical environment changes, and rates changes sign, simply because 1000mM are harder to remove per time interval than just 1mM.

As a consequence, we wish to point out that the model was applied for the first time on a big dataset. It is unlikely that the parameter estimation from one clone was so universal that it is valid for future, novel data under all kinds of different chemical conditions. But as soon as new clones are available, a new fit can and should be made by specifying upper and lower limits to all concentrations so that future simulations will lie within physiologically reasonable boundaries of the new dataset. To demonstrate this, we show exemplarily how a factor of 10 in enzyme level of PFK can lead to unphysiological F1,6bP concentrations for two clones above 60 and 900 mM. This could potentially happen when transcript level and isoform composition push one or several rates multiplicatively to such values.

4. Discussion

4.1. Insights from simulations

Our simulations showed that two parameters played a pivotal role in mammalian metabolism: i) the way glucose flux and concentration is controlled and the timing, and ii) power and direction of pH shifts. Both parameters are thus considered critical process parameters in QbD jargon [98][59][99] and can change the course of a fermentation significantly. The effect of pHi on pHe can help to explain some effects, such as reduced growth or flux under more acidic conditions, and comparison between extremely low with extremely high conditions may appear to have a high impact on flux, however, in our simulation we have shown that using a very reasonable pHi adaptation to pHe results in approximately 7-9% in flux increase or decrease per each 0,2 units of pHe which matters when the pH is prone to strong fluctuations such as at the beginning of a batch cultivation until the first 48h where the pH can easily encompass a shift of 0,6 units, (i.e. from 7,4 to 6,8). As a consequence, pH can influence both the equilibrium between lactic acid and H⁺ ions in and outside the cell [100]. Its effect on internal enzymes is pivotal in describing a modulation of glycolytic flux and why pH shifts are simple means to reduce or prevent overflow metabolism [39].

4.2. Link to predictive process control

Ensuring the cell's metabolic demands has been a playground for engineers for decades [84][101] and continues to be both interesting and relevant to industry even today. But the desire for developing a process with the highest final titer is challenging [25][102][103]. To stay competitive, companies have to focus on reducing the unexplainable sources of variability, and one of them is the pH profile. Lactic acid, aeration strategy, feed and medium composition all share part of the blame. It is well known that being able to hold pH without adding control reagents like CO₂ or base is a challenge not many are willing or able to accept in fed-batch cultivations.

However, controlling flux and lactic acid build-up is one very potent way to ensure a consistent pH profile, which will in turn affects important parameters such as product quality, productivity, growth rate

and viability of the culture and potentially prolong cultivation time [104]. The intricate relationship between pH_i and pH_e may become easier to handle which in turn allows a better description of intracellular pH dependencies such as key glycolytic enzymes [42][69].

Conclusively, our simulations were conducted under two industrially relevant process modes: limitation and non-limited conditions. Both conditions were probed with pH shifts and showed to have an effect on lactic acid concentration at the time of glucose pulsing. Growth rate was shown to be dependent on timing and intensity of the process events due to a transient reduction of lactic acid build-up. However, care must be taken of the assumptions about growth. We use a very simple relationship of glucose limitation and lactic acid inhibition to describe the growth rate, which is not as simple as that in real life. In principle our assumption holds true for some process modes, but it is prone to artifacts. One such artifact was demonstrated by imposing a very low glycolytic flux, and as a consequence having no active metabolism but large growth. We therefore ask the operators to consider that only an active metabolism can make growth possible.

4.3. Link to holistic cell line engineering

Variation in isoform can be explored in depth as was demonstrated with LDH and lead to cues and ideas for improved cell line engineering, both by trying to overexpress, knock-out or modify any participating enzyme. Our results show that apart from the usual suspects HK, PFK and PK also differences in LDH isoforms [105] are worth closer inspection as they affect more directly lactic acid equilibrium inside and outside the cells. With bigger and more accurate datasets, less known enzymes may turn out to play an important part in the overall metabolic response. We therefore hypothesize that these genes might be promising targets for epigenetic engineering in future efforts to prevent lactic acid accumulation and growth inhibition.

Most genes in glycolysis are well-known in the field for years, but their differential expression leads to new cues and leverage to fine-tune metabolism *in silico* [62]. The knowledge of detailed metabolic mechanisms has already been partially integrated in constructing improved cell lines for bioprocess development which produce less lactic acid, even without a reduced glucose environment. Still, most genetic backgrounds can be further refined, for instance by making them more robust towards otherwise negative process events such as pH or even too large substrate shifts by integrating isoforms usually found in other tissues [106][107][108] which are more tolerant towards high glucose already by nature.

4.4. Link to directed protein design

Examples for successful protein engineering which has led to a favorable metabolic behavior is seldom loudly broadcasted because it represents years of research and knowledge that had to accumulate, be maintained by generations of scientist and brought to success in private and industrial research labs. However, we hope to shed some light on the process technological consequences of engineering efforts and show how metabolism as a whole is affected by a change in parameters of LDH, HK, PK or PFK.

Researchers are willing to go the long way of knock-out mutants and cycles of clone development to test the effect of different overexpression of certain particular isoforms, which end up in the wet lab for testing. Our modeling tool may be of use to visualize the mechanistic behavior prior to stepping into a laboratory and run experiments under a variety of conditions which may be used to gather important knowledge. We are aware that a satisfactory model takes a long time to develop, but we believe that even our current reduced model representing only the crudest glycolysis pathways in 13 reactions is enough to shed some light on allosteric loops which affect a culture's metabolism under norm conditions like in a bioreactor greatly. Later wet-lab experiments should then be easier to set up to draw the most out of the consequences of an alteration in the genetic code of mammalian cells [109]. We hope that future engineering efforts can be modularly extended to consider the results of simulations under a variety of cultivation conditions and process modes. As logical consequence, targeted protein design will become more important in the future and this tool might assist in speeding up bioprocess development as a whole.

5. Conclusions

This contribution shows that linking traditional technologies with each other may have several benefits over their isolated observation. First, we recreate mammalian cell culture metabolism in an artificial mathematical environment. Then, we simulated metabolic behavior under glucose limited and non-limited conditions with pH shifts of different intensity and timing. The *in silico* results show that both have a distinct effect on lactic acid profiles and also on growth. We wish to point out that metabolism can be highly clone-dependent and that our model parameters must first be recalibrated to represent internal metabolites more accurately in their physiological range. After this, two clones which behave very differently should be picked for a validation of the modified model. While we do not have these clones ready to run in our hands, we believe that this contribution is valuable to gather process knowledge outside the lab.

This model can be readily calibrated to one particular clone by changing the parameters of interest and used to explore different process control or protein engineering consequences on the metabolism. Several process modes can be set up, from batch, fed-batch or pulse-feeding scenarios to controlled limitations or pH shifts. Many unwanted and unexpected side-effects and additional complexity can be simply ruled out because the variance in the outcome of the simulations has one defined source: the variation of a parameter in the model.

In this synthetic environment, we were able to observe clone-specific differences when different genetic background, but also different process conditions are set up in a series of scenarios to test the clone's metabolic performance. It was shown that not just one, but several strategies can lead to a strong reduction in a clone's lactic acid formation in culture. This plethora of individual strategies allows for tremendous synergies, therefore they can and should be linked in order to discover the most favorable cultivation conditions for future clones.

6. Outlook

This contribution was one of the first steps to show how several disciplines can be bridged in a systems approach to explain glycolytic behavior in mammalian cell culture. We are still at the beginning to grasp the consequences of cell engineering on metabolism. Few attempts were made at all to combine related, yet so distant fields as process control and clone design. Our contribution has focused on how to integrate protein-specific substrate specificity, genetic distribution of isoforms and process control by pH shifts or glucose pulsing into one platform to make a qualitative statement about the clone's future metabolic behavior. Real wet lab verification might therefore encompass the same shifts in pH or pulses of glucose in and outside glucose-limited conditions for two opposite clones.

In our simulations, two clones had a very distinct lactic acid metabolism *in silico*. These clones were A8MAB and A11PARA, and they showed different behavior in a series of different scenarios. However, the clones are not available in our lab and we would have to expose two industrial strains to exactly the same conditions, involving proprietary medium and feed compositions. We may or may not be able to obtain the same epigenetic response if we deviate from the clone's natural cultivation conditions. Further efforts should be therefore directed to in-house clone analysis, simulation and prediction to make a really independent qualitative statement about the capabilities of this model.

List of Abbreviations

<i>A11PARA</i>	Clone 1
<i>A8MAB</i>	Clone 2
<i>ALDO</i>	Aldolase
<i>CA</i>	Concentration of compound A
<i>Ccf26p</i>	Cytosolic concentration of fructose-2,6-bisphosphate
<i>Ccf6p</i>	Cytosolic concentration of fructose-6-phosphate
<i>Ccfbp</i>	Cytosolic concentration of fructose-1,6-bisphosphate
<i>Cegl</i>	Extracellular concentration of glucose
<i>Celac</i>	Extracellular concentration of lactic acid
<i>ENO</i>	Enolase
<i>F6P</i>	Fructose-6-phosphate
<i>F1,6bP</i>	Fructose-1,6-bisphosphate
<i>F2,6bP</i>	Fructose-2,6-bisphosphate
<i>FAC</i>	Isoform factor
<i>GAPDH</i>	Glyceraldehyde 3-Phosphate Dehydrogenase
<i>GCK</i>	Glucokinase, HK IV
<i>GLC</i>	Glucose
<i>GPI</i>	Glucose Phosphate Isomerase
<i>HK</i>	Hexokinase
<i>K, Km</i>	Michaelis menten constant
<i>LAC</i>	Lactic acid

<i>LDH</i>	Lactate Dehydrogenase
<i>MCT</i>	Mono Carboxylate Transporter
<i>my</i>	Growth rate
<i>N</i>	Denominator in rate equations
<i>PFK</i>	Phosphofructokinase
<i>PFKFB</i>	6-Phosphofructo-2-Kinase/Fructose-2,6-Bisphosphatase
<i>PGK</i>	Phosphoglycerate Kinase
<i>PGM</i>	Phosphoglycerate Mutase
<i>pHe</i>	External pH
<i>pHi</i>	Internal (cytosolic) pH
<i>PK</i>	Pyruvate Kinase
<i>qglc</i>	Specific glucose uptake rate
<i>qlac</i>	Specific lactic acid production/consumption rate
<i>rbw</i>	Backward reaction
<i>r fw</i>	Forward reaction
<i>rHK</i>	Rate of HK
<i>rmax</i>	Maximum rate
<i>SLCxxax</i>	Solute Carrier, MCT
<i>TPI</i>	Triose Phosphate Isomerase
<i>TSL</i>	Transcript level factor
<i>VCC</i>	Viable Cell Concentration

Concentrations in mM, rates in mM/h, VCC in E5/ml, my in h⁻¹ unless stated otherwise.

Acknowledgments

Financial support by the Marshall Plan Foundation is gratefully acknowledged. Bhanu Mulukutla is hereby kindly acknowledged for authoring the very first code lines of the mathematical model, without whom this work would not have been possible. The CEMS team at the University of Minnesota is thanked for being supportive, kind and cheerful during the whole duration of the scientific exchange.

Author Contributions

VK designed and performed the simulations, wrote the manuscript, prepared tables, figures and adapted the source code for the simulations, TL helped to explain the mathematical aspects of the code for simulations, gave valuable advice, helped with critical discussions of modeling aspects and was a good comrade during the whole time of the project and beyond, AY shared his code, literature and additional information regarding the mathematical model, RR and NV provided transcriptomic data for integration into the mathematical model, CH supervised and reviewed critically the manuscript, WH supervised, instructed, critically reviewed the manuscript, conceived the study and gave valuable support during the short research exchange at the host University.

Conflicts of Interest

The authors declare no conflict of interest.

© 2015 by the authors;

References

- [1] Y.-T. Luan, T. C. Stanek, and D. Drapeau, "Controlling lactic acid production in fed-batch cell cultures via variation in glucose concentration; bioreactors and heterologous gene expression," US7429491 B2, 30-Sep-2008.
- [2] R. Brent, "A partnership between biology and engineering," *Nat. Biotechnol.*, vol. 22, no. 10, pp. 1211–1214, Oct. 2004.
- [3] A. R. Joyce and B. O. Palsson, "Toward whole cell modeling and simulation: comprehensive functional genomics through the constraint-based approach," *Prog. Drug Res. Fortschritte Arzneimittelforschung Prog. Rech. Pharm.*, vol. 64, pp. 265, 267–309, 2007.
- [4] P. Wechselberger, P. Sagmeister, H. Engelking, T. Schmidt, J. Wenger, and C. Herwig, "Efficient feeding profile optimization for recombinant protein production using physiological information," *Bioprocess Biosyst. Eng.*, vol. 35, no. 9, pp. 1637–1649, Nov. 2012.
- [5] V. Gogvadze, B. Zhivotovsky, and S. Orrenius, "The Warburg effect and mitochondrial stability in cancer cells," *Mol. Aspects Med.*, vol. 31, no. 1, pp. 60–74, Feb. 2010.
- [6] O. Warburg, "On the origin of cancer cells," *Science*, vol. 123, no. 3191, pp. 309–314, Feb. 1956.
- [7] A. Yongky, J. Lee, T. Le, B. C. Mulukutla, P. Daoutidis, and W.-S. Hu, "Mechanism for multiplicity of steady states with distinct cell concentration in continuous culture of mammalian cells," *Biotechnol. Bioeng.*, p. n/a–n/a, Feb. 2015.
- [8] B. C. Mulukutla, M. Gramer, and W.-S. Hu, "On metabolic shift to lactate consumption in fed-batch culture of mammalian cells," *Metab. Eng.*, vol. 14, no. 2, pp. 138–149, Mar. 2012.
- [9] A. Lohmeier, T. Thüte, S. Northoff, J. Hou, T. Munro, and T. Noll, "Effects of perfusion processes under limiting conditions on different Chinese Hamster Ovary cells," *BMC Proc.*, vol. 7, no. Suppl 6, p. P64, Dec. 2013.
- [10] H. L. Nandita Vishwanathan, "Advancing biopharmaceutical process science through transcriptome analysis," *Curr. Opin. Biotechnol.*, vol. 30, pp. 113–119, 2014.
- [11] B. C. Mulukutla, S. Khan, A. Lange, and W.-S. Hu, "Glucose metabolism in mammalian cell culture: new insights for tweaking vintage pathways," *Trends Biotechnol.*, vol. 28, no. 9, pp. 476–484, Sep. 2010.
- [12] N. Vishwanathan, A. Yongky, K. C. Johnson, H.-Y. Fu, N. M. Jacob, H. Le, F. N. K. Yusufi, D. Y. Lee, and W.-S. Hu, "Global insights into the Chinese hamster and CHO cell transcriptomes," *Biotechnol. Bioeng.*, p. n/a–n/a, Dec. 2014.
- [13] J. Monod, J. Wyman, and J.-P. Changeux, "On the nature of allosteric transitions: A plausible model," *J. Mol. Biol.*, vol. 12, no. 1, pp. 88–118, Mai 1965.
- [14] E. Tziampazis and A. Sambanis, "Modeling of cell culture processes," *Cytotechnology*, vol. 14, no. 3, pp. 191–204, Jan. 1994.
- [15] K. K. Frame and W.-S. Hu, "Kinetic study of hybridoma cell growth in continuous culture. I. A model for non-producing cells," *Biotechnol. Bioeng.*, vol. 37, no. 1, pp. 55–64, Jan. 1991.
- [16] E. L. King and C. Altman, "A Schematic Method of Deriving the Rate Laws for Enzyme-Catalyzed Reactions," *J. Phys. Chem.*, vol. 60, no. 10, pp. 1375–1378, 1956.

- [17] M. Aehle, K. Bork, S. Schaepe, A. Kuprijanov, R. Horstkorte, R. Simutis, and A. Lübbert, "Increasing batch-to-batch reproducibility of CHO-cell cultures using a model predictive control approach," *Cytotechnology*, vol. 64, no. 6, pp. 623–634, Mar. 2012.
- [18] S. Craven, N. Shirsat, J. Whelan, and B. Glennon, "Process model comparison and transferability across bioreactor scales and modes of operation for a mammalian cell bioprocess," *Biotechnol. Prog.*, vol. 29, no. 1, pp. 186–196, 2013.
- [19] B. Romein, "Mathematical modelling of mammalian cells in suspension culture," *Delft University of Technology*. [Online]. Available: <http://www.tnw.tudelft.nl/en/about-faculty/departments/biotechnology/research-groups/cell-systems-engineering/research-projects/romein/>. [Accessed: 22-Nov-2013].
- [20] N. Vriezen, B. Romein, K. C. A. M. Luyben, and J. P. van Dijken, "Effects of glutamine supply on growth and metabolism of mammalian cells in chemostat culture," *Biotechnol. Bioeng.*, vol. 54, no. 3, pp. 272–286, 1997.
- [21] G. W. Hiller, D. S. Clark, and H. W. Blanch, "Cell retention-chemostat studies of hybridoma cells—analysis of hybridoma growth and metabolism in continuous suspension culture in serum-free medium," *Biotechnol. Bioeng.*, vol. 42, no. 2, pp. 185–195, Jun. 1993.
- [22] H. Niu, Z. Amribt, P. Fickers, W. Tan, and P. Bogaerts, "Metabolic pathway analysis and reduction for mammalian cell cultures—Towards macroscopic modeling," *Chem. Eng. Sci.*, vol. 102, pp. 461–473, Oktober 2013.
- [23] C. . Sanderson, J. . Barford, and G. . Barton, "A structured, dynamic model for animal cell culture systems," *Biochem. Eng. J.*, vol. 3, no. 3, pp. 203–211, Jun. 1999.
- [24] Z. Amribt, H. Niu, and P. Bogaerts, "Macroscopic modelling of overflow metabolism and model based optimization of hybridoma cell fed-batch cultures," *Biochem. Eng. J.*, vol. 70, pp. 196–209, Jan. 2013.
- [25] J. O. Basch, S. Gangloff, C. E. Joosten, D. Kothari, S. S. Lee, K. Leister, L. Matlock, S. Sakhamuri, B. M. Schilling, and S. G. Zegarelli, "Product quality enhancement in mammalian cell culture processes for protein production," WO2004058944 A2, 15-Jul-2004.
- [26] M. K. Jeon, D. Y. Yu, and G. M. Lee, "Combinatorial engineering of ldh-a and bcl-2 for reducing lactate production and improving cell growth in dihydrofolate reductase-deficient Chinese hamster ovary cells," *Appl. Microbiol. Biotechnol.*, vol. 92, no. 4, pp. 779–790, Nov. 2011.
- [27] J. C. Rathmell, C. J. Fox, D. R. Plas, P. S. Hammerman, R. M. Cinalli, and C. B. Thompson, "Akt-directed glucose metabolism can prevent Bax conformation change and promote growth factor-independent survival," *Mol. Cell. Biol.*, vol. 23, no. 20, pp. 7315–7328, Oct. 2003.
- [28] M. B. Burg, J. D. Ferraris, and N. I. Dmitrieva, "Cellular Response to Hyperosmotic Stresses," *Physiol. Rev.*, vol. 87, no. 4, pp. 1441–1474, Oct. 2007.
- [29] F. Franěk and K. Šrámková, "Cell suicide in starving hybridoma culture: survival-signal effect of some amino acids," *Cytotechnology*, vol. 21, no. 1, pp. 81–89, Jan. 1996.
- [30] R. Pörtner and T. Schäfer, "Modelling hybridoma cell growth and metabolism — a comparison of selected models and data," *J. Biotechnol.*, vol. 49, no. 1–3, pp. 119–135, Aug. 1996.
- [31] "METHOD FOR CONTROLLING pH, OSMOLALITY AND DISSOLVED CARBON DIOXIDE LEVELS IN A MAMMALIAN CELL CULTURE PROCESS TO ENHANCE CELL VIABILITY AND BIOLOGIC PRODUCT YIELD."
- [32] M. M. Zhu, A. Goyal, D. L. Rank, S. K. Gupta, T. V. Boom, and S. S. Lee, "Effects of Elevated pCO₂ and Osmolality on Growth of CHO Cells and Production of Antibody-Fusion Protein B1: A Case Study," *Biotechnol. Prog.*, vol. 21, no. 1, pp. 70–77, 2005.
- [33] R. W. Hutkins and N. L. Nannen, "pH Homeostasis in Lactic Acid Bacteria," *J. Dairy Sci.*, vol. 76, no. 8, pp. 2354–2365, Aug. 1993.
- [34] W. F. Boron, "Regulation of intracellular pH," *Adv. Physiol. Educ.*, vol. 28, no. 1–4, pp. 160–179, Dec. 2004.

- [35] J. A. Cook and M. H. Fox, "Effects of chronic pH 6.6 on growth, intracellular pH, and response to 42.0 degrees C hyperthermia of Chinese hamster ovary cells," *Cancer Res.*, vol. 48, no. 9, pp. 2417–2420, May 1988.
- [36] G. L'Allemain, S. Paris, and J. Pouysségur, "Growth factor action and intracellular pH regulation in fibroblasts. Evidence for a major role of the Na⁺/H⁺ antiport.," *J. Biol. Chem.*, vol. 259, no. 9, pp. 5809–5815, May 1984.
- [37] M. Ivarsson, T. K. Villiger, M. Morbidelli, and M. Soos, "Evaluating the impact of cell culture process parameters on monoclonal antibody N-glycosylation," *J. Biotechnol.*, vol. 188C, pp. 88–96, Aug. 2014.
- [38] E. Trummer, K. Fauland, S. Seidinger, K. Schriebl, C. Lattenmayer, R. Kunert, K. Vorauer-Uhl, R. Weik, N. Borth, H. Katinger, and D. Müller, "Process parameter shifting: Part I. Effect of DOT, pH, and temperature on the performance of Epo-Fc expressing CHO cells cultivated in controlled batch bioreactors," *Biotechnol. Bioeng.*, vol. 94, no. 6, pp. 1033–1044, Aug. 2006.
- [39] M. Ivarsson, H. Noh, M. Morbidelli, and M. Soos, "Insights into pH-induced metabolic switch by flux balance analysis," *Biotechnol. Prog.*, p. n/a–n/a, Jan. 2015.
- [40] S. Oguchi, H. Saito, M. Tsukahara, and H. Tsumura, "pH Condition in temperature shift cultivation enhances cell longevity and specific hMab productivity in CHO culture," *Cytotechnology*, vol. 52, no. 3, pp. 199–207, Nov. 2006.
- [41] M. Magnani, V. Stocchi, N. Serafini, E. Piatti, M. Dachà, and G. Fornaini, "Pig red blood cell hexokinase: Regulatory characteristics and possible physiological role," *Arch. Biochem. Biophys.*, vol. 226, no. 1, pp. 377–387, Oct. 1983.
- [42] M. Magnani, V. Stocchi, G. Serafini, and M. Bossù, "Effects of buffers and pH on rabbit red blood cell hexokinase," *Ital. J. Biochem.*, vol. 32, no. 1, pp. 28–35, Feb. 1983.
- [43] P. J. Mulquiney and P. W. Kuchel, "Model of the pH-dependence of the concentrations of complexes involving metabolites, haemoglobin and magnesium ions in the human erythrocyte," *Eur. J. Biochem. FEBS*, vol. 245, no. 1, pp. 71–83, Apr. 1997.
- [44] P. J. Mulquiney and P. W. Kuchel, "Model of 2,3-bisphosphoglycerate metabolism in the human erythrocyte based on detailed enzyme kinetic equations: equations and parameter refinement," *Biochem. J.*, vol. 342, no. Pt 3, pp. 581–596, Sep. 1999.
- [45] R. Rekhi and A. A. Qutub, "Systems approaches for synthetic biology: a pathway toward mammalian design," *Comput. Physiol. Med.*, vol. 4, p. 285, 2013.
- [46] H. Kitano, "Systems biology: a brief overview," *Science*, vol. 295, no. 5560, pp. 1662–1664, Mar. 2002.
- [47] R. Feeney, A. R. Clarke, and J. J. Holbrook, "A single amino acid substitution in lactate dehydrogenase improves the catalytic efficiency with an alternative coenzyme," *Biochem. Biophys. Res. Commun.*, vol. 166, no. 2, pp. 667–672, Jan. 1990.
- [48] F. Züllli, R. Schneiter, R. Urfer, and H. Zuber, "Structure and function of L-lactate dehydrogenases from thermophilic and mesophilic bacteria, XI. Engineering thermostability and activity of lactate dehydrogenases from bacilli," *Biol. Chem. Hoppe. Seyler*, vol. 372, no. 5, pp. 363–372, May 1991.
- [49] B. C. Mulukutla, A. Yongky, P. Daoutidis, and W.-S. Hu, "Bistability in Glycolysis Pathway as a Physiological Switch in Energy Metabolism," *PLoS ONE*, vol. 9, no. 6, p. e98756, Jun. 2014.
- [50] The UniProt Consortium, "UniProt: a hub for protein information," *Nucleic Acids Res.*, Oct. 2014.
- [51] U. Wittig, R. Kania, M. Golebiewski, M. Rey, L. Shi, L. Jong, E. Algaa, A. Weidemann, H. Sauer-Danzwith, S. Mir, O. Krebs, M. Bittkowski, E. Wetsch, I. Rojas, and W. Müller, "SABIO-RK--database for biochemical reaction kinetics," *Nucleic Acids Res.*, vol. 40, no. Database issue, pp. D790–796, Jan. 2012.
- [52] N. Paczia, A. Nilgen, T. Lehmann, J. Gätgens, W. Wiechert, and S. Noack, "Extensive exometabolome analysis reveals extended overflow metabolism in various microorganisms," *Microb. Cell Factories*, vol. 11, no. 1, p. 122, Sep. 2012.
- [53] H. J. Cruz, J. L. Moreira, and M. J. Carrondo, "Metabolic shifts by nutrient manipulation in continuous cultures of BHK cells," *Biotechnol. Bioeng.*, vol. 66, no. 2, pp. 104–113, 1999.

- [54] A. F. Europa, A. Gambhir, P.-C. Fu, and W.-S. Hu, "Multiple steady states with distinct cellular metabolism in continuous culture of mammalian cells," *Biotechnol. Bioeng.*, vol. 67, no. 1, pp. 25–34, Jan. 2000.
- [55] P. M. O'Callaghan and D. C. James, "Systems biotechnology of mammalian cell factories," *Brief. Funct. Genomic. Proteomic.*, vol. 7, no. 2, pp. 95–110, Mar. 2008.
- [56] G. Seth, S. Charaniya, K. F. Wlaschin, and W.-S. Hu, "In pursuit of a super producer—alternative paths to high producing recombinant mammalian cells," *Curr. Opin. Biotechnol.*, vol. 18, no. 6, pp. 557–564, Dezember 2007.
- [57] O. Spadiut, S. Rittmann, C. Dietzsch, and C. Herwig, "Dynamic process conditions in bioprocess development," *Eng. Life Sci.*, vol. 13, no. 1, pp. 88–101, 2013.
- [58] J. E. Dowd, K. E. Kwok, and J. M. Piret, "Glucose-based optimization of CHO-cell perfusion cultures," *Biotechnol. Bioeng.*, vol. 75, no. 2, pp. 252–256, Oct. 2001.
- [59] D. M. J. D. Jesus, M. Bourgeois, G. Baumgartner, P. Tromba, D. M. Jordan, M. H. Amstutz, and P. F. M. Wurm, "The Influence of pH on Cell Growth and Specific Productivity of Two CHO Cell Lines Producing Human Anti Rh D IgG," in *Animal Cell Technology: From Target to Market*, D. E. Lindner-Olsson, M. N. Chatzissavidou, and D. E. Lüllau, Eds. Springer Netherlands, 2001, pp. 197–199.
- [60] M. Gagnon, G. Hiller, Y.-T. Luan, A. Kittredge, J. DeFelice, and D. Drapeau, "High-End pH-controlled delivery of glucose effectively suppresses lactate accumulation in CHO Fed-batch cultures," *Biotechnol. Bioeng.*, vol. 108, no. 6, pp. 1328–1337, 2011.
- [61] C. D. Smolke and P. A. Silver, "Informing biological design by integration of systems and synthetic biology," *Cell*, vol. 144, no. 6, pp. 855–859, Mar. 2011.
- [62] N. Y. Oparina, A. V. Snezhkina, A. F. Sadritdinova, V. A. Veselovskii, A. A. Dmitriev, V. N. Senchenko, N. V. Mel'nikova, A. S. Speranskaya, M. V. Darii, O. A. Stepanov, I. M. Barkhatov, and A. V. Kudryavtseva, "[Differential expression of genes that encode glycolysis enzymes in kidney and lung cancer in humans]," *Genetika*, vol. 49, no. 7, pp. 814–823, Jul. 2013.
- [63] K. Sikand, J. Singh, J. S. Ebron, and G. C. Shukla, "Housekeeping Gene Selection Advisory: Glyceraldehyde-3-Phosphate Dehydrogenase (GAPDH) and β -Actin Are Targets of miR-644a," *PLoS ONE*, vol. 7, no. 10, p. e47510, Oct. 2012.
- [64] A. Yalcin, B. F. Clem, Y. Imbert-Fernandez, S. C. Ozcan, S. Peker, J. O'Neal, A. C. Klarer, A. L. Clem, S. Telang, and J. Chesney, "6-Phosphofructo-2-kinase (PFKFB3) promotes cell cycle progression and suppresses apoptosis via Cdk1-mediated phosphorylation of p27," *Cell Death Dis.*, vol. 5, p. e1337, 2014.
- [65] S. Vora, R. Oskam, and G. E. Staal, "Isoenzymes of phosphofructokinase in the rat. Demonstration of the three non-identical subunits by biochemical, immunochemical and kinetic studies," *Biochem. J.*, vol. 229, no. 2, pp. 333–341, Jul. 1985.
- [66] T. A. Rapoport, R. Heinrich, and S. M. Rapoport, "The regulatory principles of glycolysis in erythrocytes in vivo and in vitro. A minimal comprehensive model describing steady states, quasi-steady states and time-dependent processes.," *Biochem. J.*, vol. 154, no. 2, pp. 449–469, Feb. 1976.
- [67] J. E. Wilson, "Isozymes of mammalian hexokinase: structure, subcellular localization and metabolic function," *J. Exp. Biol.*, vol. 206, no. 12, pp. 2049–2057, Jun. 2003.
- [68] L. Miccoli, S. Oudard, F. Sureau, F. Poirson, B. Dutrillaux, and M. F. Poupon, "Intracellular pH governs the subcellular distribution of hexokinase in a glioma cell line.," *Biochem. J.*, vol. 313, no. Pt 3, pp. 957–962, Feb. 1996.
- [69] I. Auzat, G. Le Bras, P. Branny, F. De La Torre, B. Theunissen, and J. R. Garel, "The role of Glu187 in the regulation of phosphofructokinase by phosphoenolpyruvate," *J. Mol. Biol.*, vol. 235, no. 1, pp. 68–72, Jan. 1994.
- [70] B. Trivedi and W. H. Danforth, "Effect of pH on the kinetics of frog muscle phosphofructokinase," *J. Biol. Chem.*, vol. 241, no. 17, pp. 4110–4112, Sep. 1966.
- [71] J. J. Osman, J. Birch, and J. Varley, "The response of GS-NS0 myeloma cells to pH shifts and pH perturbations," *Biotechnol. Bioeng.*, vol. 75, no. 1, pp. 63–73, Oct. 2001.

- [72] S. S. Ozturk and B. O. Palsson, "Growth, metabolic, and antibody production kinetics of hybridoma cell culture: 2. Effects of serum concentration, dissolved oxygen concentration, and medium pH in a batch reactor," *Biotechnol. Prog.*, vol. 7, no. 6, pp. 481–494, Dec. 1991.
- [73] N. Kurano, C. Leist, F. Messi, S. Kurano, and A. Fiechter, "Growth behavior of Chinese hamster ovary cells in a compact loop bioreactor: 1. Effects of physical and chemical environments," *J. Biotechnol.*, vol. 15, no. 1–2, pp. 101–111, Jul. 1990.
- [74] J. P. B. J. D. Jang, "Effect of feed rate on growth rate and antibody production in the fed-batch culture of murine hybridoma cells," *Cytotechnology*, vol. 32, no. 3, 2000.
- [75] K. Fischer, P. Hoffmann, S. Voelkl, N. Meidenbauer, J. Ammer, M. Edinger, E. Gottfried, S. Schwarz, G. Rothe, S. Hoves, K. Renner, B. Timischl, A. Mackensen, L. Kunz-Schughart, R. Andreesen, S. W. Krause, and M. Kreutz, "Inhibitory effect of tumor cell-derived lactic acid on human T cells," *Blood*, vol. 109, no. 9, pp. 3812–3819, May 2007.
- [76] L. Xie, G. Nyberg, X. Gu, H. Li, F. Möllborn, and D. I. Wang, "Gamma-interferon production and quality in stoichiometric fed-batch cultures of Chinese hamster ovary (CHO) cells under serum-free conditions," *Biotechnol. Bioeng.*, vol. 56, no. 5, pp. 577–582, Dec. 1997.
- [77] V. Singh, "On-line measurement of oxygen uptake in cell culture using the dynamic method," *Biotechnol. Bioeng.*, vol. 52, no. 3, pp. 443–448, 1996.
- [78] K. Eyer, A. Oeggerli, and E. Heinzle, "On-line gas analysis in animal cell cultivation: II. Methods for oxygen uptake rate estimation and its application to controlled feeding of glutamine," *Biotechnol. Bioeng.*, vol. 45, no. 1, pp. 54–62, 1995.
- [79] P. Ducommun, P.-A. Ruffieux, M.-P. Furter, I. Marison, and U. von Stockar, "A new method for on-line measurement of the volumetric oxygen uptake rate in membrane aerated animal cell cultures," *J. Biotechnol.*, vol. 78, no. 2, pp. 139–147, März 2000.
- [80] S. Ansorge, G. Esteban, C. Ghommidh, and G. Schmid, "Monitoring Nutrient Limitations by Online Capacitance Measurements in Batch & Fed-batch CHO Fermentations," in *Cell Technology for Cell Products*, R. Smith, Ed. Springer Netherlands, 2007, pp. 723–726.
- [81] J. E. Dowd, A. Jubb, K. E. Kwok, and J. M. Piret, "Optimization and control of perfusion cultures using a viable cell probe and cell specific perfusion rates," *Cytotechnology*, vol. 42, no. 1, pp. 35–45, May 2003.
- [82] T. Noll and M. Biselli, "Dielectric spectroscopy in the cultivation of suspended and immobilized hybridoma cells," *J. Biotechnol.*, vol. 63, no. 3, pp. 187–198, Aug. 1998.
- [83] A. M. Jobé, C. Herwig, M. Surzyn, B. Walker, I. Marison, and U. von Stockar, "Generally applicable fed-batch culture concept based on the detection of metabolic state by on-line balancing," *Biotechnol. Bioeng.*, vol. 82, no. 6, pp. 627–639, Jun. 2003.
- [84] S. S. Ozturk, J. C. Thrift, J. D. Blackie, and D. Naveh, "Real-time monitoring and control of glucose and lactate concentrations in a mammalian cell perfusion reactor," *Biotechnol. Bioeng.*, vol. 53, no. 4, pp. 372–378, 1997.
- [85] H. P. J. Bonarius, C. D. de Gooijer, J. Tramper, and G. Schmid, "Determination of the respiration quotient in mammalian cell culture in bicarbonate buffered media," *Biotechnol. Bioeng.*, vol. 45, no. 6, pp. 524–535, 1995.
- [86] M. Jenzsch, S. Gnoth, M. Kleinschmidt, R. Simutis, and A. Lübbert, "Improving the batch-to-batch reproducibility of microbial cultures during recombinant protein production by regulation of the total carbon dioxide production," *J. Biotechnol.*, vol. 128, no. 4, pp. 858–867, März 2007.
- [87] G. W. Gould and G. D. Holman, "The glucose transporter family: structure, function and tissue-specific expression," *Biochem. J.*, vol. 295, no. Pt 2, pp. 329–341, Oct. 1993.
- [88] W. Zhou, J. Rehm, and W.-S. Hu, "High viable cell concentration fed-batch cultures of hybridoma cells through on-line nutrient feeding," *Biotechnol. Bioeng.*, vol. 46, no. 6, pp. 579–587, 1995.
- [89] "Novel strategy to reduce lactic acid production and control ph in animal cell culture."
- [90] F. Lu, P. C. Toh, I. Burnett, F. Li, T. Hudson, A. Amanullah, and J. Li, "Automated dynamic fed-batch process and media optimization for high productivity cell culture process development," *Biotechnol. Bioeng.*, vol. 110, no. 1, pp. 191–205, 2013.

- [91] D. Chee Fung Wong, K. Tin Kam Wong, L. Tang Goh, C. Kiat Heng, and M. Gek Sim Yap, "Impact of dynamic online fed-batch strategies on metabolism, productivity and N-glycosylation quality in CHO cell cultures," *Biotechnol. Bioeng.*, vol. 89, no. 2, pp. 164–177, 2005.
- [92] R. Stambaugh and D. Post, "Substrate and Product Inhibition of Rabbit Muscle Lactic Dehydrogenase Heart (H4) and Muscle (M4) Isozymes," *J. Biol. Chem.*, vol. 241, no. 7, pp. 1462–1467, Apr. 1966.
- [93] S. Merry and H. G. Britton, "The mechanism of rabbit muscle phosphofructokinase at pH8," *Biochem. J.*, vol. 226, no. 1, pp. 13–28, Feb. 1985.
- [94] G. A. Dunaway, T. P. Kasten, T. Sebo, and R. Trapp, "Analysis of the phosphofructokinase subunits and isoenzymes in human tissues," *Biochem. J.*, vol. 251, no. 3, pp. 677–683, May 1988.
- [95] R. L. Hanson, F. B. Rudolph, and H. A. Lardy, "Rabbit muscle phosphofructokinase. The kinetic mechanism of action and the equilibrium constant," *J. Biol. Chem.*, vol. 248, no. 22, pp. 7852–7859, Nov. 1973.
- [96] M. Otto, R. Heinrich, G. Jacobasch, and S. Rapoport, "A mathematical model for the influence of anionic effectors on the phosphofructokinase from rat erythrocytes," *Eur. J. Biochem. FEBS*, vol. 74, no. 2, pp. 413–420, Apr. 1977.
- [97] M. Otto, R. Heinrich, B. Kühn, and G. Jacobasch, "A Mathematical Model for the Influence of Fructose 6-Phosphate, ATP, Potassium, Ammonium and Magnesium on the Phosphofructokinase from Rat Erythrocytes," *Eur. J. Biochem.*, vol. 49, no. 1, pp. 169–178, Nov. 1974.
- [98] S. F. Abu-Absi, L. Yang, P. Thompson, C. Jiang, S. Kandula, B. Schilling, and A. A. Shukla, "Defining process design space for monoclonal antibody cell culture," *Biotechnol. Bioeng.*, vol. 106, no. 6, pp. 894–905, 2010.
- [99] D. Zalai, C. Dietzsch, and C. Herwig, "Risk-based Process Development of Biosimilars as Part of the Quality by Design Paradigm," *PDA J. Pharm. Sci. Technol. PDA*, vol. 67, no. 6, pp. 569–580, Dec. 2013.
- [100] J. W. Locasale and L. C. Cantley, "Metabolic Flux and the Regulation of Mammalian Cell Growth," *Cell Metab.*, vol. 14, no. 4, pp. 443–451, Oktober 2011.
- [101] D. Drapeau, Y.-T. Luan, and T. C. Stanek, "Restricted glucose feed for animal cell culture," WO2004104186 A1, 02-Dec-2004.
- [102] S. D. Roger and A. Mikhail, "Biosimilars: opportunity or cause for concern?," *J. Pharm. Pharm. Sci. Publ. Can. Soc. Pharm. Sci. Société Can. Sci. Pharm.*, vol. 10, no. 3, pp. 405–410, 2007.
- [103] H. Schellekens, "Biosimilar therapeutics—what do we need to consider?," *NDT Plus*, vol. 2, no. Suppl 1, pp. i27–i36, Jan. 2009.
- [104] H. Aghamohseni, K. Ohadi, M. Spearman, N. Krahn, M. Moo-Young, J. M. Scharer, M. Butler, and H. M. Budman, "Effects of nutrient levels and average culture pH on the glycosylation pattern of camelid-humanized monoclonal antibody," *J. Biotechnol.*, vol. 186C, pp. 98–109, Jul. 2014.
- [105] W.-S. Hu, A. Kantardjieff, and B. C. Mulukutla, "Cell lines that overexpress lactate dehydrogenase c," WO2012075124 A2, 07-Jun-2012.
- [106] R. Noguchi, H. Kubota, K. Yugi, Y. Toyoshima, Y. Komori, T. Soga, and S. Kuroda, "The selective control of glycolysis, gluconeogenesis and glycogenesis by temporal insulin patterns," *Mol. Syst. Biol.*, vol. 9, p. 664, 2013.
- [107] E. W. Somberg and M. A. Mehlman, "Regulation of gluconeogenesis and lipogenesis. The regulation of mitochondrial pyruvate metabolism in guinea-pig liver synthesizing precursors for gluconeogenesis," *Biochem. J.*, vol. 112, no. 4, pp. 435–447, May 1969.
- [108] S. J. Pilkis and T. H. Claus, "Hepatic Gluconeogenesis/Glycolysis: Regulation and Structure/Function Relationships of Substrate Cycle Enzymes," *Annu. Rev. Nutr.*, vol. 11, no. 1, pp. 465–515, 1991.
- [109] N. J. Brown, S. E. Higham, B. Perunovic, M. Arafa, S. Balasubramanian, and I. Rehman, "Lactate Dehydrogenase-B Is Silenced by Promoter Methylation in a High Frequency of Human Breast Cancers," *PLoS ONE*, vol. 8, no. 2, p. e57697, Feb. 2013.

- [110] G. Gerber, H. Preissler, R. Heinrich, and S. M. Rapoport, "Hexokinase of Human Erythrocytes," *Eur. J. Biochem.*, vol. 45, no. 1, pp. 39–52, Jun. 1974.
- [111] G. Rijksen, G. Jansen, R. J. Kraaijenhagen, M. J. Van der Vlist, A. M. Vlug, and G. E. Staal, "Separation and characterization of hexokinase I subtypes from human erythrocytes," *Biochim. Biophys. Acta*, vol. 659, no. 2, pp. 292–301, Jun. 1981.
- [112] G. Rijksen and G. E. Staal, "Regulation of human erythrocyte hexokinase. The influence of glycolytic intermediates and inorganic phosphate," *Biochim. Biophys. Acta*, vol. 485, no. 1, pp. 75–86, Nov. 1977.
- [113] G. Fornaini, M. Magnani, A. Fazi, A. Accorsi, V. Stocchi, and M. Dachà, "Regulatory properties of human erythrocyte hexokinase during cell ageing," *Arch. Biochem. Biophys.*, vol. 239, no. 2, pp. 352–358, Jun. 1985.
- [114] R. W. Gracy and B. E. Tilley, "Phosphoglucose isomerase of human erythrocytes and cardiac tissue," *Methods Enzymol.*, vol. 41, pp. 392–400, 1975.
- [115] S. Kitajima, R. Sakakibara, and K. Uyeda, "Kinetic studies of fructose 6-phosphate,2-kinase and fructose 2,6-bisphosphatase," *J. Biol. Chem.*, vol. 259, no. 11, pp. 6896–6903, Jun. 1984.
- [116] M. Kretschmer, W. Schellenberger, and E. Hofmann, "Quasi-stationary concentrations of fructose-2,6-bisphosphate in the phosphofructokinase-2/fructose-2,6-bisphosphatase cycle," *Biochem. Biophys. Res. Commun.*, vol. 131, no. 2, pp. 899–904, Sep. 1985.
- [117] D. A. Okar, A. Manzano, A. Navarro-Sabatè, L. Riera, R. Bartrons, and A. J. Lange, "PFK-2/FBPase-2: maker and breaker of the essential biofactor fructose-2,6-bisphosphate," *Trends Biochem. Sci.*, vol. 26, no. 1, pp. 30–35, Jan. 2001.
- [118] S. K. Srivastava and E. Beutler, "The effect of normal red cell constituents on the activities of red cell enzymes," *Arch. Biochem. Biophys.*, vol. 148, no. 1, pp. 249–255, Jan. 1972.
- [119] E. Beutler, "2,3-diphosphoglycerate affects enzymes of glucose metabolism in red blood cells," *Nature. New Biol.*, vol. 232, no. 27, pp. 20–21, Jul. 1971.
- [120] A. H. Mehler, "Kinetic Properties of Native and Carboxypeptidase-altered Rabbit Muscle Aldolase," *J. Biol. Chem.*, vol. 238, no. 1, pp. 100–104, Jan. 1963.
- [121] A. H. Mehler and B. Bloom, "Interaction between rabbit muscle aldolase and dihydroxyacetone phosphate," *J. Biol. Chem.*, vol. 238, pp. 105–107, Jan. 1963.
- [122] E. E. Penhoet, M. Kochman, and W. J. Rutter, "Isolation of fructose diphosphate aldolases A, B, and C," *Biochemistry (Mosc.)*, vol. 8, no. 11, pp. 4391–4395, Nov. 1969.
- [123] E. E. Penhoet, M. Kochman, and W. J. Rutter, "Molecular and catalytic properties of aldolase C," *Biochemistry (Mosc.)*, vol. 8, no. 11, pp. 4396–4402, Nov. 1969.
- [124] E. Strapazon and T. L. Steck, "Interaction of the aldolase and the membrane of human erythrocytes," *Biochemistry (Mosc.)*, vol. 16, no. 13, pp. 2966–2971, Jun. 1977.
- [125] D. R. Yeltman and B. G. Harris, "Purification and characterization of aldolase from human erythrocytes," *Biochim. Biophys. Acta*, vol. 484, no. 1, pp. 188–198, Sep. 1977.
- [126] I. A. Rose, E. L. O'Connell, and A. H. Mehler, "Mechanism of the Aldolase Reaction," *J. Biol. Chem.*, vol. 240, no. 4, pp. 1758–1765, Apr. 1965.
- [127] E. Beutler, *Red Cell Metabolism: A Manual of Biochemical Methods*, 3 Sub edition. Orlando, FL: Grune & Stratton, 1984.
- [128] T. H. Sawyer, B. E. Tilley, and R. W. Gracy, "Studies on Human Triosephosphate Isomerase II. NATURE OF THE ELECTROPHORETIC MULTIPLICITY IN ERYTHROCYTES," *J. Biol. Chem.*, vol. 247, no. 20, pp. 6499–6505, Oct. 1972.
- [129] A. S. Schneider, W. N. Valentine, M. Hattori, and H. L. Heins, "Hereditary Hemolytic Anemia with Triosephosphate Isomerase Deficiency," *N. Engl. J. Med.*, vol. 272, no. 5, pp. 229–235, Feb. 1965.
- [130] O. Meyerhof and R. Junowicz-Kocholaty, "The Equilibria of Isomerase and Aldolase, and the Problem of the Phosphorylation of Glyceraldehyde Phosphate," *J. Biol. Chem.*, vol. 149, no. 1, pp. 71–92, Jul. 1943.

- [131] R. W. Gracy, "Triosephosphate isomerase from human erythrocytes," *Methods Enzymol.*, vol. 41, pp. 442–447, 1975.
- [132] C. S. Wang and P. Alaupovic, "Glyceraldehyde-3-phosphate dehydrogenase from human erythrocyte membranes. Kinetic mechanism and competitive substrate inhibition by glyceraldehyde 3-phosphate," *Arch. Biochem. Biophys.*, vol. 205, no. 1, pp. 136–145, Nov. 1980.
- [133] F. Heinz and B. Freimüller, "Glyceraldehyde-3-phosphate dehydrogenase from human tissues," *Methods Enzymol.*, vol. 89 Pt D, pp. 301–305, 1982.
- [134] C. S. Furfine and S. F. Velick, "THE ACYL-ENZYME INTERMEDIATE AND THE KINETIC MECHANISM OF THE GLYCERALDEHYDE 3-PHOSPHATE DEHYDROGENASE REACTION," *J. Biol. Chem.*, vol. 240, pp. 844–855, Feb. 1965.
- [135] C. F. Cori, S. F. Velick, and G. T. Cori, "The combination of diphosphopyridine nucleotide with glyceraldehyde phosphate dehydrogenase," *Biochim. Biophys. Acta*, vol. 4, no. 1–3, pp. 160–169, Jan. 1950.
- [136] W. K. G. Krietsch and T. Bücher, "3-Phosphoglycerate Kinase from Rabbit Sceletal Muscle and Yeast," *Eur. J. Biochem.*, vol. 17, no. 3, pp. 568–580, Dec. 1970.
- [137] A. Yoshida and S. Watanabe, "Human phosphoglycerate kinase. I. Crystallization and characterization of normal enzyme," *J. Biol. Chem.*, vol. 247, no. 2, pp. 440–445, Jan. 1972.
- [138] M. Ali and Y. S. Brownstone, "A study of phosphoglycerate kinase in human erythrocytes. II. Kinetic properties," *Biochim. Biophys. Acta*, vol. 445, no. 1, pp. 89–103, Aug. 1976.
- [139] W. J. O. C S Lee, "Properties and mechanism of human erythrocyte phosphoglycerate kinase.," *J. Biol. Chem.*, vol. 250, no. 4, pp. 1275–81, 1975.
- [140] M. P. B. W, and K. P, "Model of 2,3-bisphosphoglycerate metabolism in the human erythrocyte based on detailed enzyme kinetic equations1: in vivo kinetic characterization of 2,3-bisphosphoglycerate synthase/phosphatase using ¹³C and ³¹P NMR," 15-Sep-1999. [Online]. Available: <http://www.biochemj.org/bj/342/bj3420567.htm>. [Accessed: 16-Nov-2014].
- [141] P. J. Mulquiney and P. W. Kuchel, "Model of 2,3-bisphosphoglycerate metabolism in the human erythrocyte based on detailed enzyme kinetic equations: computer simulation and metabolic control analysis," *Biochem. J.*, vol. 342 Pt 3, pp. 597–604, Sep. 1999.
- [142] C. C. Rider and C. B. Taylor, "Enolase isoenzymes in rat tissues: Electrophoretic, chromatographic, immunological and kinetic properties," *Biochim. Biophys. Acta BBA - Protein Struct.*, vol. 365, no. 1, pp. 285–300, Sep. 1974.
- [143] F. Wold and C. E. Ballou, "Studies on the enzyme enolase. I. Equilibrium studies," *J. Biol. Chem.*, vol. 227, no. 1, pp. 301–312, Jul. 1957.
- [144] L. Garfinkel and D. Garfinkel, "Magnesium regulation of the glycolytic pathway and the enzymes involved," *Magnesium*, vol. 4, no. 2–3, pp. 60–72, 1985.
- [145] H. G. Holzhütter, G. Jacobasch, and A. Bisdorff, "Mathematical modelling of metabolic pathways affected by an enzyme deficiency. A mathematical model of glycolysis in normal and pyruvate-kinase-deficient red blood cells," *Eur. J. Biochem. FEBS*, vol. 149, no. 1, pp. 101–111, May 1985.
- [146] J. F. Koster, R. G. Slee, G. E. Staal, and T. J. van Berkel, "The influence of glucose 1,6-diphosphate on the enzymatic activity of pyruvate kinase," *Biochim. Biophys. Acta*, vol. 258, no. 3, pp. 763–768, Mar. 1972.
- [147] S. Ainsworth and N. Macfarlane, "A kinetic study of rabbit muscle pyruvate kinase," *Biochem. J.*, vol. 131, no. 2, pp. 223–236, Feb. 1973.
- [148] A. Kahn and J. Marie, "Pyruvate kinases from human erythrocytes and liver," *Methods Enzymol.*, vol. 90 Pt E, pp. 131–140, 1982.
- [149] K. R. Albe, M. H. Butler, and B. E. Wright, "Cellular concentrations of enzymes and their substrates," *J. Theor. Biol.*, vol. 143, no. 2, pp. 163–195, Mar. 1990.
- [150] E. Rozengurt, L. J. de Asúa, and H. Carminatti, "Some Kinetic Properties of Liver Pyruvate Kinase (Type L) II. EFFECT OF pH ON ITS ALLOSTERIC BEHAVIOR," *J. Biol. Chem.*, vol. 244, no. 12, pp. 3142–3147, Jun. 1969.

- [151] V. Zewe and H. J. Fromm, "Kinetic Studies of Rabbit Muscle Lactate Dehydrogenase. II. Mechanism of the Reaction*," *Biochemistry (Mosc.)*, vol. 4, no. 4, pp. 782–792, Apr. 1965.
- [152] U. Borgmann, T. W. Moon, and K. J. Laidler, "Molecular kinetics of beef heart lactate dehydrogenase," *Biochemistry (Mosc.)*, vol. 13, no. 25, pp. 5152–5158, Dec. 1974.
- [153] C. S. Wang, "Inhibition of human erythrocyte lactate dehydrogenase by high concentrations of pyruvate. Evidence for the competitive substrate inhibition," *Eur. J. Biochem. FEBS*, vol. 78, no. 2, pp. 569–574, Sep. 1977.
- [154] M. Uldry and B. Thorens, "The SLC2 family of facilitated hexose and polyol transporters," *Pflüg. Arch. Eur. J. Physiol.*, vol. 447, no. 5, pp. 480–489, Feb. 2004.
- [155] A. P. Halestrap and D. Meredith, "The SLC16 gene family—from monocarboxylate transporters (MCTs) to aromatic amino acid transporters and beyond," *Pflüg. Arch. Eur. J. Physiol.*, vol. 447, no. 5, pp. 619–628, Feb. 2004.
- [156] C. Juel and A. P. Halestrap, "Lactate transport in skeletal muscle — role and regulation of the monocarboxylate transporter," *J. Physiol.*, vol. 517, no. Pt 3, pp. 633–642, Jun. 1999.

Appendix

This appendix is based on the appendices of [7][49], and unpublished work under review by Yongky et al. with a few optional additions which can be activated or deactivated in the code of the model.

Rate equations

Kinetic rate equations for all the enzymes used in the model have all been previously derived mechanistically and reported in various literature. This section describes these kinetic equations for all the enzymes considered. The steady state kinetics for all the enzymes were based on the King and Altman method [16] employing the known mechanisms and regulations. The rate equations for the enzymes phosphofructokinase (PFK) and pyruvate kinase (PK) employ the Monod-Wyman-Changeux method [13] to model the allosteric effects of various metabolite modulators. Kinetic constants used in the rate equations of the current model were experimentally determined values and obtained from previously reported studies.

Glycolysis

Hexokinase (HK): The rate equation for HK was taken from Mulquiney et al. [44]. The kinetic constants which correspond to those of the isozyme HK2 were adopted from previous literature [110]–[113]. The rate equation employs the partial rapid equilibrium random bi bi mechanism, which is a simplification of the steady state random bi bi system with the assumption that except for the reactive-ternary complexes, all the other steps in the mechanism are fast reactions. The inhibitions by G6P, glucose-1,6-phosphate (G16BP), 2,3-bisphosphoglycerate (23BPG) and glutathione (GSH) were modeled as mixed type of inhibition affecting both the activity (V_{\max}) as well as the affinity (K_M) of the enzyme for glucose.

$$r_{HK} = \left(V_{mf}^{HK} \frac{C_{MgATP}^c C_{GLC}^c}{K_{MgATP}^{HK} K_{GLC}^{HK}} - V_{mr}^{HK} \frac{C_{MgADP}^c C_{G6P}^c}{K_{i,MgADP}^{HK} K_{G6P}^{HK}} \right) \frac{1}{N_{HK}}$$

$$N_{HK} = \left(1 + \frac{C_{MgATP}^c}{K_{i,MgATP}^{HK}} + \frac{C_{G6P}^c}{K_{i,G6P}^{HK}} + \frac{C_{GLC}^c}{K_{GLC}^{HK}} + \frac{C_{MgATP}^c C_{GLC}^c}{K_{MgATP}^{HK} K_{GLC}^{HK}} + \frac{C_{MgADP}^c}{K_{i,MgADP}^{HK}} + \frac{C_{MgADP}^c C_{G6P}^c}{K_{i,MgADP}^{HK} K_{G6P}^{HK}} \right. \\ \left. + \frac{C_{GLC}^c C_{G6P}^c}{K_{GLC}^{HK} K_{G6P}^{HK}} + \frac{C_{GLC}^c C_{G16BP}^c}{K_{GLC}^{HK} K_{i,G16BP}^{HK}} + \frac{C_{GLC}^c C_{23BPG}^c}{K_{GLC}^{HK} K_{i,23BPG}^{HK}} + \frac{C_{GLC}^c C_{GSH}^c}{K_{GLC}^{HK} K_{i,GSH}^{HK}} \right)$$

$$V_{mf}^{HK} = 6.38 * 10^3 \text{ mM h}^{-1}$$

$$V_{mr}^{HK} = 41 \text{ mM h}^{-1}$$

$$K_{MgATP}^{HK} = 1.0 \text{ mM}$$

$$K_{GLC}^{HK} = 0.1 \text{ mM}$$

$$K_{i,MgADP}^{HK} = 1.0 \text{ mM}$$

$$K_{G6P}^{HK} = 0.47 \text{ mM}$$

$$K_{i,G6P}^{HK} = 0.47 \text{ mM}$$

$$K_{i,G16BP}^{HK} = 0.03 \text{ mM}$$

$$K_{i,GSH}^{HK} = 3.0 \text{ mM}$$

$$K_{i,23BPG}^{HK} = 4.0 \text{ mM}$$

Glucose Phosphate Isomerase (GPI): The rate equation for GPI was taken from Mulquiney et al. [44].

The kinetic constants were adopted from previous literature [114]. The rate equation employs the steady state uni uni reaction kinetics.

$$r_{GPI} = \frac{V_{mf}^{GPI} \frac{C_{G6P}^c}{K_f^{GPI}} - V_{mr}^{GPI} \frac{C_{F6P}^c}{K_r^{GPI}}}{1 + \frac{C_{G6P}^c}{K_f^{GPI}} + \frac{C_{F6P}^c}{K_r^{GPI}}}$$

$$V_{mf}^{GPI} = 4.8 * 10^4 \text{ mM h}^{-1}$$

$$V_{mr}^{GPI} = 4.0 * 10^4 \text{ mM h}^{-1}$$

$$K_f^{GPI} = 0.3 \text{ mM}$$

$$K_r^{GPI} = 0.123 \text{ mM}$$

Phosphofructokinase (PFK): The rate equation for PFK was taken from Mulquiney et al. [44]. The

kinetic constants were adopted from previous literature [93]–[97]. The rate kinetics was based on the two state allosteric model using ordered bi bi mechanism. The two state model considers that the enzyme can exist in the active or the non-active state as determined by the levels of the activity modulators. These include activators (F6P, F16BP, F26BP, G16BP, AMP etc) and inhibitors (ATP, Mg etc). Some of these activity modulators act on all the isozymes of PFK while others are isozyme specific. For example, F6P acts as a substrate as well as an allosteric activator for all the isozymes of PFK, whereas F16BP only stimulates PFKM and PFKL. The fraction of enzyme in the active state is represented by the nonlinear term N_{PFK} which is a function of the levels of the activity modulators. L_{PFK} represents the equilibrium constant between the two states of the enzyme in the absence of any substrates. The initial velocity expression for the enzyme fraction in the active state was modeled as partial rapid equilibrium random bi bi steady state equation similar to the HK kinetics.

$$r_{PFK} = \frac{\frac{V_f^{PFK} C_{MgATP}^c C_{F6P}^c}{K_{F6P}^{PFK} K_{MgATP}^{PFK}} - \frac{V_r^{PFK} C_{MgADP}^c C_{F16BP}^c}{K_{F16BP}^{PFK} K_{MgADP}^{PFK}}}{\left(\left(1 + \frac{C_{F6P}^c}{K_{F6P}^{PFK}} \right) \left(1 + \frac{C_{MgATP}^c}{K_{MgATP}^{PFK}} \right) + \left(1 + \frac{C_{F16BP}^c}{K_{F16BP}^{PFK}} \right) \left(1 + \frac{C_{MgADP}^c}{K_{MgADP}^{PFK}} \right) - 1 \right)} N_{PFK}$$

$$N_{PFK} = 1 + \frac{L_{PFK} \left(1 + \frac{C_{ATP}^c}{K_{ATP}^{PFK}} \right)^4 \left(1 + \frac{C_{Mg}^c}{K_{Mg}^{PFK}} \right)^4 \left(1 + \frac{C_{2,3BPG}^c}{K_{2,3BPG}^{PFK}} \right)^4}{\left(1 + \frac{C_{F6P}^c}{K_{F6P}^{PFK}} + \frac{C_{F16BP}^c}{K_{F16BP}^{PFK}} \right)^4 \left(1 + \frac{C_{AMP}^c}{K_{AMP}^{PFK}} \right)^4 \left(1 + \frac{C_{G16BP}^c}{K_{G16BP}^{PFK}} \right)^4 \left(1 + \frac{C_{Pi}^c}{K_{Pi}^{PFK}} \right)^4 \left(1 + \frac{C_{F26BP}^c}{K_{F26BP}^{PFK}} \right)^4}$$

$$V_f^{PFK} = 15.5 * 10^2 \text{ mM}^{-1} \text{ h}^{-1}$$

$$V_r^{PFK} = 6.78 * 10^1 \text{ mM}^{-1} \text{ h}^{-1}$$

$$K_{F6P}^{PFK} = 6 * 10^{-2} \text{ mM}$$

$$K_{MgATP}^{PFK} = 6.8 * 10^{-2} \text{ mM}$$

$$K_{MgADP}^{PFK} = 0.54 \text{ mM}$$

$$K_{F16BP}^{PFK} = 0.65 \text{ mM}$$

$$K_{F26BP}^{PFK} = 5.5 * 10^{-3} \text{ mM}$$

$$K_{G16BP}^{PFK} = 0.1 \text{ mM}$$

$$K_{ATP}^{PFK} = 0.1 \text{ mM}$$

$$K_{AMP}^{PFK} = 0.3 \text{ mM}$$

$$K_{Mg}^{PFK} = 0.2 \text{ mM}$$

$$K_{Pi}^{PFK} = 30 \text{ mM}$$

$$K_{23BPG}^{PFK} = 0.5 \text{ mM}$$

$$L_{PFK} = 2 * 10^{-3}$$

6-Phosphofructo-2-Kinase/Fructose-2,6-Bisphosphatase (PFKFB): The rate equation for PFKFB and the kinetic constants were taken from previously reported studies [115][116]. PFKFB is a bi-functional enzyme with kinase and bisphosphatase activities, each localized to either terminals of the enzyme and are independent of each other's activity. The kinase domain catalyzes the synthesis of fructose-2,6-bisphosphate (F26BP) from fructose-6-phosphate (F6P) and the bisphosphatase domain mediates the hydrolysis of F26BP to F6P. The reaction kinetics for the kinase domain (r_{PFK2}) follows the ordered bi bi steady state kinetics, with phosphoenolpyruvate (PEP) inhibition of the kinase domain modeled as non-competitive inhibition. The bisphosphatase reaction kinetics ($r_{F2,6BPase}$) was modeled as simple Michaelis-Menten kinetics with non-competitive product inhibition by F6P. Isozymes of PFKFB vary in their kinase to bisphosphatase activity (K/P) [117]. The effect of isozyme (or K/P) was modeled by changing the Vmax of r_{PFK2} and holding $r_{F2,6BPase}$ constant.

$$r_{PFK2} = \frac{V_{f,PFK2} \left(C_{ATP}^c C_{F6P}^c - \frac{C_{ADP}^c C_{F26BP}^c}{K_{eq,PFK2}} \right)}{\left(K_{i,ATP}^{PFK2} K_{m,F6P}^{PFK2} + K_{m,F6P}^{PFK2} C_{ATP}^c + K_{m,ATP}^{PFK2} C_{F6P}^c + \frac{K_{m,ADP}^{PFK2} C_{F26BP}^c}{K_{eq,PFK2}} + \frac{K_{m,F26BP}^{PFK2} C_{ADP}^c}{K_{eq,PFK2}} \right) + C_{ATP}^c C_{F6P}^c + \frac{K_{m,ADP}^{PFK2} C_{ATP}^c C_{F26BP}^c}{K_{eq,PFK2} K_{i,ATP}^{PFK2}} + \frac{C_{ADP}^c C_{F26BP}^c}{K_{eq,PFK2}} + \frac{K_{m,ATP}^{PFK2} C_{ADP}^c C_{F6P}^c}{K_{i,ADP}^{PFK2}} + \frac{C_{ATP}^c C_{F6P}^c C_{F26BP}^c}{K_{i,F26BP}^{PFK2}} + \frac{C_{ADP}^c C_{F6P}^c C_{F26BP}^c}{K_{eq,PFK2} K_{i,F6P}^{PFK2}} \left(1 + \frac{C_{PEP}^c}{K_{i,PEP}^{PFK2}} \right)$$

$$r_{F2,6BPase} = \frac{V_{F2,6BPase} C_{F26BP}^c}{\left(1 + \frac{C_{F6P}^c}{K_{i,F6P}^{F2,6BPase}} \right) \left(K_{m,F26BP}^{F2,6BPase} + C_{F26BP}^c \right)}$$

$$V_{f,PFK2} = 41.6 \text{ mM h}^{-1}$$

$$K_{m,ATP}^{PFK2} = 0.15 \text{ mM}$$

$$K_{m,F6P}^{PFK2} = 0.032 \text{ mM}$$

$$K_{m,F26BP}^{PFK2} = 0.008 \text{ mM}$$

$$K_{m,ADP}^{PFK2} = 0.062 \text{ mM}$$

$$K_{i,ATP}^{PFK2} = 0.15 \text{ mM}$$

$$K_{i,F6P}^{PFK2} = 0.001 \text{ mM}$$

$$K_{i,F26BP}^{PFK2} = 0.02 \text{ mM}$$

$$K_{i,ADP}^{PFK2} = 0.23 \text{ mM}$$

$$K_{i,PEP}^{PFK2} = 0.013 \text{ mM}$$

$$K_{eq}^{PFK2} = 16$$

$$V_{F2,6BPase} = 11.78 \text{ mM}^{-1} \text{ h}^{-1}$$

$$K_{m,F26BP}^{F2,6BPase} = 1 * 10^{-3} \text{ mM}$$

$$K_{i,F6P}^{F2,6BPase} = 25 * 10^{-3} \text{ mM}$$

Aldolase (ALDO): The rate equation for ALDO was taken from Mulquiney et al. [44]. The kinetic constants were adopted or estimated from previous literature [118]–[127]. The reaction kinetics of ALDO follows the ordered uni bi steady state kinetics. Inhibition due to 23BPG as described in the original expression was retained in this study. However, since 23BPG is not a reaction intermediate considered in the model, its concentration was held constant for the purpose of this study.

$$r_{ALD} = \frac{\frac{V_{mf}^{ALD} C_{F16BP}^c}{K_{F16BP}^{ALD}} - \frac{V_{mr}^{ALD} C_{GAP}^c C_{DHAP}^c}{K_{GAP}^{ALD} K_{i,DHAP}^{ALD}}}{\left(1 + \frac{C_{23BPG}^c}{K_{i,23BPG}^{ALD}} + \frac{C_{F16BP}^c}{K_{F16BP}^{ALD}} + \frac{K_{DHAP}^{ALD} C_{GAP}^c}{K_{GAP}^{ALD} K_{i,DHAP}^{ALD}} \left(1 + \frac{C_{23BPG}^c}{K_{i,23BPG}^{ALD}} \right) + \frac{C_{DHAP}^c}{K_{i,DHAP}^{ALD}} + \frac{K_{DHAP}^{ALD} C_{F16BP}^c C_{GAP}^c}{K_{i,F16BP}^{ALD} K_{GAP}^{ALD} K_{i,DHAP}^{ALD}} + \frac{C_{DHAP}^c C_{GAP}^c}{K_{GAP}^{ALD} K_{i,DHAP}^{ALD}} \right)}$$

$$V_{mf}^{ALD} = 6.75 * 10^2 \text{ mM h}^{-1}$$

$$V_{mr}^{ALD} = 2.32 * 10^3 \text{ mM h}^{-1}$$

$$K_{F16BP}^{ALD} = 5 * 10^{-2} \text{ mM}$$

$$K_{i,F16BP}^{ALD} = 1.98 * 10^{-2} \text{ mM}$$

$$K_{DHAP}^{ALD} = 3.5 * 10^{-2} \text{ mM}$$

$$K_{i,DHAP}^{ALD} = 1.1 * 10^{-2} \text{ mM}$$

$$K_{GAP}^{ALD} = 0.189 \text{ mM}$$

$$K_{i,23BPG}^{ALD} = 1.5 \text{ mM}$$

Triose Phosphate Isomerase (TPI): The rate equation for TPI was taken from Mulquiney et al. [44]. The kinetic constants were adopted from previous literature [127]–[131]. The rate kinetics of TPI follows a simple steady state uni uni reaction kinetics.

$$r_{TPI} = \frac{V_{mf}^{TPI} \frac{C_{DHAP}^c}{K_f^{TPI}} - V_{mr}^{TPI} \frac{C_{GAP}^c}{K_r^{TPI}}}{1 + \frac{C_{DHAP}^c}{K_f^{TPI}} + \frac{C_{GAP}^c}{K_r^{TPI}}}$$

$$V_{mf}^{TPI} = 5.10 * 10^2 \text{ mM h}^{-1}$$

$$V_{mr}^{TPI} = 4.61 * 10^1 \text{ mM h}^{-1}$$

$$K_f^{TPI} = 1.62 * 10^{-1} \text{ mM}$$

$$K_r^{TPI} = 4.30 * 10^{-1} \text{ mM}$$

Glyceraldehyde 3-Phosphate Dehydrogenase (GAPDH): The rate equation for GAPDH was taken from Mulquiney et al. [44]. The kinetic constants were adopted from previous literature [132]–[135]. The rate kinetics of GAPDH follows the ter ter (bi uni uni bi ping pong) steady state kinetics.

$$r_{GAPD} = \frac{V_{mf}^{GAPD} \frac{C_{NAD^+}^c C_{Pi}^c C_{GAP}^c}{K_{NAD^+}^{GAPD} K_{i,Pi}^{GAPD} K_{i,GAP}^{GAPD}} - V_{mr}^{GAPD} \frac{C_{13BPG}^c C_{NADH}^c C_{H^+}^c}{K_{i,13BPG}^{GAPD} K_{NADH}^{GAPD}}}{\frac{C_{GAP}^c}{K_{i,GAP}^{GAPD}} \left(1 + \frac{C_{GAP}^c}{K_{i,GAP}^{GAPD}} \right) + \frac{C_{13BPG}^c}{K_{i,13BPG}^{GAPD}} \left(1 + \frac{C_{GAP}^c}{K_{i,GAP}^{GAPD}} \right) + \frac{K_{13BPG}^{GAPD} C_{NADH}^c C_{H^+}^c}{K_{i,13BPG}^{GAPD} K_{NADH}^{GAPD}} + \frac{K_{GAP}^{GAPD} C_{NAD^+}^c C_{Pi}^c}{K_{NAD^+}^{GAPD} K_{i,Pi}^{GAPD} K_{i,GAP}^{GAPD}} + \frac{C_{NAD^+}^c C_{GAP}^c}{K_{i,NAD^+}^{GAPD} K_{i,GAP}^{GAPD}} + \frac{C_{Pi}^c C_{GAP}^c}{K_{i,Pi}^{GAPD} K_{i,GAP}^{GAPD}} \left(1 + \frac{C_{GAP}^c}{K_{i,GAP}^{GAPD}} \right) + \frac{C_{NAD^+}^c C_{13BPG}^c}{K_{i,NAD^+}^{GAPD} K_{i,13BPG}^{GAPD}} + \frac{K_{13BPG}^{GAPD} C_{Pi}^c C_{NADH}^c C_{H^+}^c}{K_{i,Pi}^{GAPD} K_{i,13BPG}^{GAPD} K_{NADH}^{GAPD}} + \frac{C_{GAP}^c C_{NADH}^c C_{H^+}^c}{K_{i,GAP}^{GAPD} K_{i,NADH}^{GAPD}} + \frac{C_{13BPG}^c C_{NADH}^c C_{H^+}^c}{K_{i,13BPG}^{GAPD} K_{NADH}^{GAPD}} + \frac{C_{NAD^+}^c C_{Pi}^c C_{GAP}^c}{K_{NAD^+}^{GAPD} K_{i,Pi}^{GAPD} K_{i,GAP}^{GAPD}} + \frac{K_{GAP}^{GAPD} C_{NAD^+}^c C_{Pi}^c C_{13BPG}^c}{K_{i,GAP}^{GAPD} K_{NAD^+}^{GAPD} K_{i,Pi}^{GAPD} K_{i,13BPG}^{GAPD}} + \frac{C_{Pi}^c C_{GAP}^c C_{NADH}^c C_{H^+}^c}{K_{i,Pi}^{GAPD} K_{i,GAP}^{GAPD} K_{i,NADH}^{GAPD}} + \frac{C_{Pi}^c C_{13BPG}^c C_{NADH}^c C_{H^+}^c}{K_{i,13BPG}^{GAPD} K_{NADH}^{GAPD} K_{i,Pi}^{GAPD} K_{i,13BPG}^{GAPD}}$$

$$V_{mf}^{GAPD} = 5.317 * 10^3 \text{ mMh}^{-1}$$

$$V_{mr}^{GAPD} = 3.919 * 10^3 \text{ mMh}^{-1}$$

$$K_{NAD^+}^{GAPD} = 0.045 \text{ mM}$$

$$K_{i,NAD^+}^{GAPD} = 0.045 \text{ mM}$$

$$K_{Pi}^{GAPD} = 3.16 \text{ mM}$$

$$K_{i,Pi}^{GAPD} = 3.16 \text{ mM}$$

$$K_{GAP}^{GAPD} = 0.095 \text{ mM}$$

$$K_{i,GAP}^{GAPD} = 1.59 * 10^{-16} \text{ mM}$$

$$K_{i,GAP}^{GAPD} = 0.031 \text{ mM}$$

$$K_{NADH}^{GAPD} = 0.0033 \text{ mM}$$

$$K_{i,NADH}^{GAPD} = 0.01 \text{ mM}$$

$$K_{13BPG}^{GAPD} = 0.00671 \text{ mM}$$

$$K_{i,13BPG}^{GAPD} = 1.52 * 10^{-18} \text{ mM}$$

$$K_{i,13BPG}^{GAPD} = 0.001 \text{ mM}$$

$$K_{eq}^{GAPD} = 1.9 * 10^{-8}$$

Phosphoglycerate Kinase (PGK): The rate equation for PGK was taken from Mulquiney et al. [44]. The kinetic constants were adopted from previous literature [136]–[139]. The rate kinetics of PGK follows the partial rapid equilibrium random bi bi steady state kinetics.

$$r_{PGK} = \frac{V_{mf}^{PGK} \frac{C_{13BPG}^c C_{MgADP}^c}{K_{i,MgADP}^{PGK} K_{13BPG}^{PGK}} - V_{mr}^{PGK} \frac{C_{3PG}^c C_{MgATP}^c}{K_{i,MgATP}^{PGK} K_{3PG}^{PGK}}}{1 + \frac{C_{13BPG}^c}{K_{i,13BPG}^{PGK}} + \frac{C_{MgADP}^c}{K_{i,MgADP}^{PGK}} + \frac{C_{13BPG}^c C_{MgADP}^c}{K_{i,MgADP}^{PGK} K_{13BPG}^{PGK}} + \frac{C_{3PG}^c}{K_{i,3PG}^{PGK}} + \frac{C_{MgATP}^c}{K_{i,MgATP}^{PGK}} + \frac{C_{3PG}^c C_{MgATP}^c}{K_{i,MgATP}^{PGK} K_{3PG}^{PGK}}}$$

$$V_{mf}^{PGK} = 5.96 * 10^4 \text{ mM h}^{-1}$$

$$V_{mr}^{PGK} = 2.39 * 10^4 \text{ mM h}^{-1}$$

$$K_{MgADP}^{PGK} = 0.1 \text{ mM}$$

$$K_{i,MgADP}^{PGK} = 0.08 \text{ mM}$$

$$K_{13BPG}^{PGK} = 0.002 \text{ mM}$$

$$K_{i,13BPG}^{PGK} = 1.6 \text{ mM}$$

$$K_{MgATP}^{PGK} = 1 \text{ mM}$$

$$K_{i,MgATP}^{PGK} = 0.186 \text{ mM}$$

$$K_{3PG}^{PGK} = 1.1 \text{ mM}$$

$$K_{i,3PG}^{PGK} = 0.205 \text{ mM}$$

$$K_{eq}^{PGK} = 3.2 * 10^3$$

Phosphoglycerate Mutase (PGM): The rate equation for PGM was taken from Mulquiney et al. [44].

The kinetic constants were adopted from previous literature [140][141]. The rate kinetics of PGM follows the uni uni steady state kinetics.

$$r_{PGAM} = \frac{V_{mf}^{PGAM} \frac{C_{3PG}^c}{K_{3PG}^{PGAM}} - V_{mr}^{PGAM} \frac{C_{2PG}^c}{K_{2PG}^{PGAM}}}{1 + \frac{C_{3PG}^c}{K_{3PG}^{PGAM}} + \frac{C_{2PG}^c}{K_{2PG}^{PGAM}}}$$

$$V_{mf}^{PGAM} = 4.894 * 10^5 \text{ mM h}^{-1}$$

$$V_{mr}^{PGAM} = 4.395 * 10^5 \text{ mM h}^{-1}$$

$$K_{3PG}^{PGAM} = 0.168 \text{ mM}$$

$$K_{2PG}^{PGAM} = 0.0256 \text{ mM}$$

$$K_{eq}^{PGAM} = 0.17$$

Enolase (ENO): The rate equation for ENO was taken from Mulquiney et al. [44]. The kinetic constants were adopted from previous literature [142][143][144]. The rate kinetics of ENO follows the partial rapid equilibrium random bi bi steady state kinetics.

$$r_{ENO} = \frac{V_{mf}^{ENO} \frac{C_{2PG}^c C_{Mg}^c}{K_{i,Mg}^{ENO} K_{2PG}^{ENO}} - V_{mr}^{ENO} \frac{C_{PEP}^c C_{Mg}^c}{K_{i,Mg}^{ENO} K_{PEP}^{ENO}}}{1 + \frac{C_{2PG}^c}{K_{i,2PG}^{ENO}} + \frac{C_{Mg}^c}{K_{i,Mg}^{ENO}} + \frac{C_{2PG}^c C_{Mg}^c}{K_{i,Mg}^{ENO} K_{2PG}^{ENO}} + \frac{C_{PEP}^c}{K_{i,PEP}^{ENO}} + \frac{C_{Mg}^c}{K_{i,Mg}^{ENO}} + \frac{C_{PEP}^c C_{Mg}^c}{K_{i,Mg}^{ENO} K_{PEP}^{ENO}}}$$

$$V_{mf}^{ENO} = 2.106 * 10^4 \text{ mM h}^{-1}$$

$$V_{mr}^{ENO} = 5.542 * 10^3 \text{ mM h}^{-1}$$

$$K_{i,Mg}^{ENO} = K_{Mg}^{ENO} = 0.14 \text{ mM}$$

$$K_{PEP}^{ENO} = K_{PEP}^{ENO} = 0.11 \text{ mM}$$

$$K_{2PG}^{ENO} = K_{2PG}^{ENO} = 0.046 \text{ mM}$$

$$K_{eq}^{ENO} = 3.0$$

Pyruvate Kinase (PK): The rate equation for PK was taken from Mulquiney et al. [44]. The kinetic constants were adopted from previous literature [145], [145]–[150]. Like PFK, the rate kinetics of PK was based on the two state allosteric model using the ordered bi bi mechanism. The two state model considers that the enzyme can exist in active or non-active state determined by the levels of the activity modulators. These include activators (F16BP, PEP, PYR etc) and inhibitors (ATP, ALA etc). The fraction of the enzyme in the active state is represented by the nonlinear term N_{PK} which is a function of levels of activity modulators. L_{PK} represents the equilibrium constant between enzymes at the two states in the absence of any substrates. The initial velocity expression for the enzyme fraction in the active state is modeled as partial rapid equilibrium random bi bi steady state equation.

$$r_{PK} = \left(\frac{V_{mf}^{PK} \frac{C_{PEP}^c}{K_{PEP}^{PK}} \frac{C_{MgADP}^c}{K_{MgADP}^{PK}} - V_{mr}^{PK} \frac{C_{PYR}^c}{K_{PYR}^{PK}} \frac{C_{MgATP}^c}{K_{MgATP}^{PK}}}{\left(I + \frac{C_{PEP}^c}{K_{PEP}^{PK}} \right) \left(I + \frac{C_{MgADP}^c}{K_{MgADP}^{PK}} \right) + \left(I + \frac{C_{PYR}^c}{K_{PYR}^{PK}} \right) \left(I + \frac{C_{MgATP}^c}{K_{MgATP}^{PK}} \right) - I} \right) \frac{I}{N_{PK}}$$

$$N_{PK} = I + L_{PK} \frac{\left(I + \frac{C_{ATP}^c}{K_{ATP}^{PK}} \right)^4 \left(I + \frac{C_{ALA}^c}{K_{ALA}^{PK}} \right)^4}{\left(I + \frac{C_{PEP}^c}{K_{PEP}^{PK}} + \frac{C_{PYR}^c}{K_{PYR}^{PK}} \right)^4 \left(I + \frac{C_{F16BP}^c}{K_{F16BP}^{PK}} + \frac{C_{G16BP}^c}{K_{G16BP}^{PK}} \right)^4}$$

$$V_{mf}^{PK} = 2.02 * 10^4 \text{ mM h}^{-1}$$

$$V_{mr}^{PK} = 47.5 \text{ mM h}^{-1}$$

$$K_{PEP}^{PK} = 2.25 * 10^{-1} \text{ mM}$$

$$K_{MgADP}^{PK} = 4.74 * 10^{-1} \text{ mM}$$

$$K_{MgATP}^{PK} = 3 \text{ mM}$$

$$K_{ATP}^{PK} = 3.39 \text{ mM}$$

$$K_{PYR}^{PK} = 4 \text{ mM}$$

$$K_{F16BP}^{PK} = 0.04 \text{ mM}$$

$$K_{G16BP}^{PK} = 1.0 * 10^{-1} \text{ mM}$$

$$L_{PK} = 0.398$$

$$K_{ALA}^{PK} = 0.02 \text{ mM}$$

Lactate Dehydrogenase (LDH): The rate equation for LDH and the kinetic constants were adopted from previous literature [44][151]–[153]. The kinetics of LDH was modeled as ordered bi bi steady state kinetics, with substrate inhibition by pyruvate.

$$r_{LDH} = \frac{V_{mf}^{LDH} \frac{C_{NADH}^c C_{PYR}^c}{K_{i,NADH}^{LDH} K_{PYR}^{LDH}} - V_{mr}^{LDH} \frac{C_{NAD}^c C_{LAC}^c}{K_{i,NAD}^{LDH} K_{LAC}^{LDH}}}{\left(1 + \frac{K_{NADH}^{LDH} C_{PYR}^c}{K_{i,NADH}^{LDH} K_{PYR}^{LDH}} + \frac{K_{NAD}^{LDH} C_{LAC}^c}{K_{i,NAD}^{LDH} K_{LAC}^{LDH}}\right) \left(1 + \frac{C_{PYR}^c}{K_{i,PYR}^{LDH}}\right) + \frac{C_{NADH}^c}{K_{i,NADH}^{LDH}} + \frac{C_{NAD}^c}{K_{i,NAD}^{LDH}} + \frac{C_{NADH}^c C_{PYR}^c}{K_{i,NADH}^{LDH} K_{PYR}^{LDH}} + \frac{K_{NAD}^{LDH} C_{NADH}^c C_{LAC}^c}{K_{i,NAD}^{LDH} K_{i,NADH}^{LDH} K_{LAC}^{LDH}} + \frac{K_{NADH}^{LDH} C_{NAD}^c C_{PYR}^c}{K_{i,NAD}^{LDH} K_{i,NADH}^{LDH} K_{PYR}^{LDH}} + \frac{C_{NAD}^c C_{LAC}^c}{K_{i,NAD}^{LDH} K_{LAC}^{LDH}} + \frac{C_{NADH}^c C_{PYR}^c C_{LAC}^c}{K_{i,NADH}^{LDH} K_{PYR}^{LDH} K_{i,LAC}^{LDH}} + \frac{C_{NAD}^c C_{PYR}^c C_{LAC}^c}{K_{i,NAD}^{LDH} K_{i,PYR}^{LDH} K_{LAC}^{LDH}}}$$

$$V_{mf}^{LDH} = 8.66 * 10^3 \text{ mM h}^{-1}$$

$$V_{mr}^{LDH} = 2.17 * 10^3 \text{ mM h}^{-1}$$

$$K_{PYR}^{LDH} = 0.137 \text{ mM}$$

$$K_{i,PYR}^{LDH} = 0.228 \text{ mM}$$

$$K_{NAD}^{LDH} = 0.107 \text{ mM}$$

$$K_{i,NAD}^{LDH} = 0.503 \text{ mM}$$

$$K_{LAC}^{LDH} = 1.07 \text{ mM}$$

$$K_{i,LAC}^{LDH} = 7.33 \text{ mM}$$

$$K_{i,NADH}^{LDH} = 5.45 * 10^{-3} \text{ mM}$$

$$K_{NADH}^{LDH} = 7.43 * 10^{-3} \text{ mM}$$

$$K_{i,PYR}^{LDH} = 0.101 \text{ mM}$$

Transport

Glucose Transporter (GLUT): Glucose transporters mediate transport of glucose across plasma membranes. Till date, fourteen glucose transporters (isozymes) have been identified which perform the same function but have very different kinetic properties [154]. Kinetics of the GLUT1 isozyme was considered in the model and was modeled as uni uni steady state kinetics.

$$r_{GLUT} = \frac{V_{mf}^{GLUT} \frac{C_{GLC}^e}{K_{GLC}^{GLUT}} - V_{mr}^{GLUT} \frac{C_{GLC}^c}{K_{GLC}^{GLUT}}}{1 + \frac{C_{GLC}^e}{K_{GLC}^{GLUT}} + \frac{C_{GLC}^c}{K_{GLC}^{GLUT}}}$$

$$V_{mf}^{GLUT} = 7.67 \text{ mMh}^{-1}$$

$$V_{mr}^{GLUT} = 0.767 \text{ mMh}^{-1}$$

$$K_{GLC}^{GLUT} = 1.50 \text{ mM}$$

Mitochondrial Pyruvate Transporter: Rate equation for pyruvate transport into mitochondrion was modeled as reversible first ordered mass kinetics.

$$r_{PYRH} = V_{mf}^{PYRH} \left(C_{PYR}^c C_{H^+}^c - C_{PYR}^m C_{H^+}^m \right)$$

$$V_{mf}^{PYRH} = 6.67 * 10^{12} \text{ mM}^{-1} \text{ h}^{-1}$$

Mono Carboxylate Transporter (MCT)

The kinetics of MCT was modeled as ordered bi bi mechanism. The kinetic constants for MCT were adopted from [155] and [156].

$$r_{MCT} = \frac{V_{m,MCT} (C_{H^+}^c C_{lac}^c - C_{H^+}^e C_{lac}^e)}{K_{m,laci}^{MCT} K_{i,H^+}^{MCT} + K_{m,H^+}^{MCT} C_{lac}^c + K_{m,laci}^{MCT} C_{H^+}^c + K_{m,H^+}^{MCT} C_{lac}^e + K_{m,laci}^{MCT} C_{H^+}^e + C_{H^+}^c C_{lac}^c} \\ C_{H^+}^e C_{lac}^e + \frac{K_{m,H^+}^{MCT} C_{lac}^c C_{H^+}^e}{K_{i,H^+}^{MCT}} + \frac{K_{m,H^+}^{MCT} C_{lac}^e C_{H^+}^c}{K_{i,H^+}^{MCT}} + \frac{C_{lac}^c C_{H^+}^c C_{H^+}^e}{K_{ii,H^+}^{MCT}} + \frac{C_{lac}^e C_{H^+}^e C_{H^+}^c}{K_{ii,H^+}^{MCT}}$$

$$V_{MCT} = 2.73 * 10^3 \text{ mM}^{-1} \text{ h}^{-1} \\ K_{m,H^+}^{MCT} = 10^{-4} \text{ mM} \\ K_{m,laci}^{MCT} = 2.5 \text{ mM} \\ K_{i,H^+}^{MCT} = 2 * 10^{-4} \text{ mM} \\ K_{ii,H^+}^{MCT} = 2 * 10^{-4} \text{ mM}$$

$P_{ATP} = 1 + \frac{C_{H^+}^m}{K_{HATP}} + \frac{C_{Mg}^m}{K_{MgATP}} + \frac{C_K^m}{K_{KATP}}$	$K_{HATP} = 2.57 * 10^{-7} M$
$P_{ADP} = 1 + \frac{C_{H^+}^m}{K_{HADP}} + \frac{C_{Mg}^m}{K_{MgADP}} + \frac{C_K^m}{K_{KADP}}$	$K_{MgATP} = 1.51 * 10^{-4} M$
$P_{AMP} = 1 + \frac{C_{H^+}^m}{K_{HAMP}} + \frac{C_{Mg}^m}{K_{MgAMP}} + \frac{C_K^m}{K_{KAMP}}$	$K_{KATP} = 1.35 * 10^{-2} M$
$P_{GTP} = P_{ATP}$	$K_{HADP} = 3.8 * 10^{-7} M$
$P_{GDP} = P_{ADP}$	$K_{MgADP} = 1.62 * 10^{-3} M$
$P_{CoASH} = 1 + \frac{C_{H^+}^m}{K_{HCoASH}}$	$K_{KADP} = 2.95 * 10^{-2} M$
$P_{cit} = 1 + \frac{C_{H^+}^m}{K_{Hcit}} + \frac{C_{Mg}^m}{K_{Mgcit}} + \frac{C_K^m}{K_{Kcit}}$	$K_{HAMP} = 6.03 * 10^{-7} M$
$P_{scoa} = 1 + \frac{C_{H^+}^m}{K_{Hscoa}}$	$K_{MgAMP} = 1.38 * 10^{-2} M$
$P_{fATP} = 1 + \frac{C_{H^+}^m}{K_{fHATP}} + \frac{C_{K^+}^m}{K_{fKATP}}$	$K_{KAMP} = 8.91 * 10^{-2} M$
$P_{fADP} = 1 + \frac{C_{H^+}^m}{K_{fHADP}} + \frac{C_{K^+}^m}{K_{fKADP}}$	$K_{HCoASH} = 7.41 * 10^{-9} M$
$P_{fAMP} = 1 + \frac{C_{H^+}^m}{K_{fHAMP}} + \frac{C_{K^+}^m}{K_{fKAMP}}$	$K_{Hcit} = 2.34 * 10^{-6} M$
$P_{fGTP} = P_{fATP}$	$K_{Mgcit} = 4.27 * 10^{-4} M$
$P_{fGDP} = P_{fADP}$	$K_{Kcit} = 4.58 * 10^{-1} M$
	$K_{Hscoa} = 1.1 * 10^{-4} M$

Mathematical model

The mathematical model for the cellular metabolism consists of material balance equations for each reaction intermediates in glycolysis. The reaction equations are from the mechanistic equations shown in the previous section. The dilution effect on metabolite concentrations caused by the cell growth was neglected considering the difference of at least one order of magnitude between the time constant for growth and specific glucose consumption rate.

$$1. \text{ Glucose: } \frac{dC_{GLC}^c}{dt} = r_{GLUT} - r_{HK}$$

$$2. \text{ Glucose 6-phosphate: } \frac{dC_{G6P}^c}{dt} = r_{HK} - r_{GPI}$$

$$3. \text{ Fructose 6-phosphate: } \frac{dC_{F6P}^c}{dt} = r_{GPI} - r_{PFK} - r_{PFK2} + r_{F2,6BPase}$$

$$4. \text{ Fructose 1,6-bisphosphate: } \frac{dC_{F16BP}^c}{dt} = r_{PFK} - r_{ALD}$$

$$5. \text{ Fructose 2,6-bisphosphate: } \frac{dC_{F26BP}^c}{dt} = r_{PFK2} - r_{F2,6BPase}$$

$$6. \text{ Dihydroxyacetone phosphate: } \frac{dC_{DHAP}^c}{dt} = r_{ALD} - r_{TPI}$$

$$7. \text{ Glyceraldehyde 3-phosphate: } \frac{dC_{GAP}^c}{dt} = r_{ALD} + r_{TPI} - r_{GAPD}$$

$$8. \text{ 1,3-bisphosphoglycerate: } \frac{dC_{13BPG}^c}{dt} = r_{GAPD} - r_{PGK}$$

$$9. \text{ 3-phosphoglycerate: } \frac{dC_{3PG}^c}{dt} = r_{PGK} - r_{PGM}$$

$$10. \text{ 2-phosphoglycerate: } \frac{dC_{2PG}^c}{dt} = r_{PGM} - r_{EN}$$

11. Phosphoenolpyruvate: $\frac{dC_{PEP}^c}{dt} = r_{EN} - r_{PK}$

12. Pyruvate: $\frac{dC_{PYR}^c}{dt} = r_{PK} - r_{LDH} - r_{PYRH}$

13. Lactate: $\frac{dC_{lac}^c}{dt} = r_{LDH} - r_{MCT}$